Large-scale manufacturing of solid-state electrolytes: Challenges, progress, and prospects

MINKIEWICZ, Justyna, JONES, Gareth M., GHANIZADEH, Shaghayegh, BOSTANCHI, Samira, WASELY, Thomas J., YAMINI, Sima Aminorroaya and NEKOUIE, Vahid <http://orcid.org/0000-0003-4335-8160>

Large-scale Manufacturing of Solid-State Electrolytes: Challenges, Progress, and Prospects

Justyna Minkiewicz [a], Gareth M. Jones [a], Shaghayegh Ghanizadeh [b], Samira Bostanchi [a], Thomas J. Wasely [b], Sima Aminorroaya Yamini [c], Vahid Nekouie [d, e]

[a] Lucideon Ltd., Stoke-on-Trent, ST4 7LQ, UK

[b] The Manufacturing Technology Centre (MTC) Limited, Ansty Park, Coventry, CV7 9JU, UK

[c] Centre for Microscopy and Microanalysis, University of Queensland, St. Lucia, Qld 4072, Australia.

[d] Department of Engineering and Mathematics, Sheffield Hallam University, Sheffield, S1 1WB, UK

[e] Materials and Engineering Research Institute, Sheffield Hallam University, Sheffield, S1 1WB, UK

Corresponding Author: Vahid Nekouie, Department of Engineering and Mathematics, Sheffield Hallam University, Sheffield, S1 1WB, UK; Materials and Engineering Research Institute, Sheffield Hallam University, Sheffield, S1 1WB, UK; Email: v.nekouie@shu.ac.uk

Abstract

Solid-state electrolytes (SSEs) are vital components in solid-state lithium batteries, which hold significant promise for energy storage applications. This review provides an overview of solid-state batteries (SSBs) and discusses the classification of electrolytes, with a focus on the challenges associated with oxide- and sulphide-based SSEs, particularly concerning interfaces and chemical stability. This review also explores methods employed to form and sinter SSEs in large-scale manufacturing, including both established and novel techniques for producing dense oxide- and sulphide-based films. Additionally, the potential application of additive manufacturing (AM) in SSE production is discussed. Lastly, the paper summarises the mass manufacturing of SSEs and provides an outlook for sustainable SSB development goals. The insights presented in this review contribute to the understanding and progress of SSE technology for solid-state lithium batteries.

Keywords: Solid-state electrolytes, Large-scale manufacturing, Forming, Sintering, Additive Manufacturing

1 Introduction

The constant push and commitment to achieve net zero greenhouse gas emissions by 2050 [1], and a growing number of electrical vehicles (EVs) on roads, have led to increased research and development (R&D) in the battery space. Electrification is crucial for achieving zero emissions and realising ambitions to decarbonise transportation. However, the rising number of EVs on roads necessitates increased energy storage capacity, extended lifespan, and fast recharging rate [2,3]. Currently, the slow charging rate hampers the adoption of EVs among potential customers, while, the development of fast-charging batteries has proven to be achievable [4].

The large-scale fabrication of solid-state batteries (SSBs) is one of the major challenges of battery technology [5]. The development of SSBs is mainly driven by the need for high-performance, rechargeable, reliable, and safe batteries. Conventional Li-ion battery technology based on a liquid, organic electrolyte has reached its performance limits of energy density, safety, and lifespan [6]. Research into SSBs requires long-term plans and is high risk, yet a foreseen method to generate opportunities and take a step toward unlocking a previously unknown potential for future electrification of the transportation sector [3–6].

Conventional Li-ion batteries use liquid or polymer gel electrolytes, while SSBs use a solid electrolyte, removing the need for a separator [4,5]. The solid-state electrolyte (SSE) can be either oxide-, sulphide-, polymer-based, or hybrid [6]. SSBs have higher energy densities and hold the potential to be safer when damaged compared to conventional Li-ion batteries [7]. High energy density and low risk of thermal runaway can possibly be achieved by coupling SSEs with a lithium (Li) metal anode in the system [8,9]. However, chemical incompatibility, electrochemical stability, interface performance, and scalability must be addressed. As the SSE is in contact with both electrodes, the choice of the suitable electrolyte is a critical parameter in the design of SSBs. In addition to chemical stability, the electrolyte must be mechanically stable and resistant to the formation of lithium dendrites [10].

Most recently published reviews tend to focus on a single processing method such as wet-chemical (e.g. sol-gel processing), vacuum-based deposition methods (e.g. CVD, PVD, ALD) for fabrication of thin films [11], Additive Manufacturing (AM) techniques and their advantages over the traditional SSE manufacturing methods [12], or they present an overview on the scientific challenges, mechanisms, and design strategies for SSBs, specifically focusing on the stability issues related to SSEs and interfaces [13].

Forming is a significant limiting factor in large-scale manufacturing of SSBs, demanding constant innovation for continuous improvements throughout the manufacturing process [14,15]. Here, we focus on the potential manufacturing routes of dense oxide- and sulphide-based SSEs, summarising their electrochemical and chemical stability, interface challenges, compatibility with binders and solvents, and possible dry or wet forming methods for large-scale manufacturing. We also evaluate the possibility of co-sintering the electrolyte and cathode together as a strategy to improve interfacial contact. Further discussion summarises potential future avenues for enhancing the large-scale manufacturing of SSE-based batteries.

2 Solid State Battery Technologies:

2.1 Overview of SSBs

Batteries based on liquid organic electrolytes, fall short in meeting demands from automotive industries due to the need for a higher rate of charge/discharge, better safety, higher energy density (350-500 Wh kg^{-1}), and potentially lower cost [14]. SSBs have been studied with the aim of addressing ongoing challenges within the EVs industry [15], such as charging time, driving range, safety, and longevity of batteries [16].

The typical structure of an SSB consists of a cathode, SSE, anode, and current collectors. A major focus is on developing high ionically conductive SSEs, which are the key components used to replace liquid electrolytes in traditional batteries [17–21]. Regarding SSEs, there are now options available in inorganic materials (oxides or sulphides), polymeric materials, and hybrids, all with bulk resistivities approaching or matching liquid electrolytes [22,23].

There are two types of configurations for SSBs: bipolar and pellet-type (Figure 1). In the former, both electrodes are coated on the end sides of the current collectors. This can result in lower weight and volume of the package and higher energy density of the batteries [18–20,24]. In the latter configuration, one layer of each of the electrodes and the SSE are stacked in a sandwich structure, which leads to lower energy density than the bipolar type, as the layers of the electrodes are thinner compared to the thick layer of SSEs. Currently, research efforts [25] to enhance SSBs are primarily focused on the pellet-type configuration. This configuration is favoured due to its less complex manufacturing process, making it suitable for in-depth studies regarding SSB advancement.

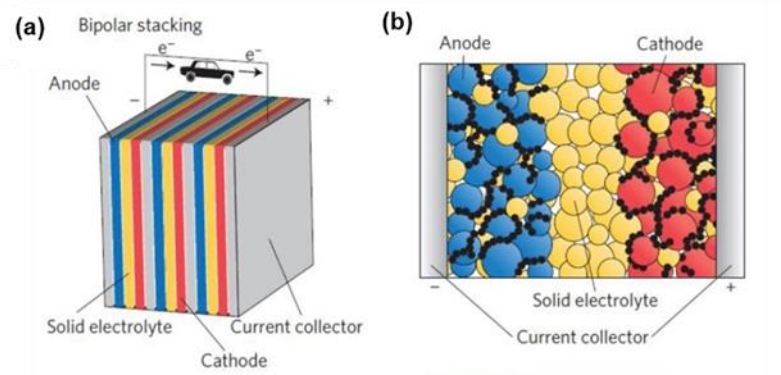

Figure 1. (a) A bipolar configuration of ASSLIBs, (b) a pellet-type configuration of SSBs. Adapted from [14].

2.2 Solid-state electrolyte (SSE) classification

All solid-state electrolytes are categorized as solid polymer electrolytes (SPEs), inorganic solid-state electrolytes (SSEs), or hybrid solid electrolytes (HSEs). Inorganic solid electrolytes are divided into oxide-based and sulphide-based electrolytes. A combination of high ionic conductivity and low electronic conductivity is necessary for the SSE to enable higher charging-discharging rates and to prevent premature failure of the battery cell. It has been established that SSEs should have a high ionic conductivity of at least 1 mS cm^{-1} [26]. However, the measured ionic conductivity of a solid material depends on many factors including properties such as lattice parameters, particle size, density, and measurement parameters such as temperature, relaxation time, and frequency. Inconsistency in reporting and lack of comparative data calls for a need to establish a common standard to measure ionic conductivity [27].

SPEs are composed of lithium (Li) or sodium (Na) salts dispersed into a polymer matrix, usually polyethylene oxide (PEO). For the past four decades, SPEs have emerged as promising candidates for SBBs because of their flexibility and ease of manufacturing [12]. However, SPEs exhibit low ionic conductivities of 10^{-8}~10^{-5} S cm^{-1} at ambient temperature and high interfacial resistance, preventing their practical use in batteries [28,29].

Inorganic SSEs are classified as glass-ceramic and crystalline electrolytes [30]. Based on the crystallographic structure, glass-ceramic and crystalline oxide-based electrolytes can be further divided into 3 groups: NASICON-type (Li $(Al,Ti)_2(PO_4)_3$, LATP), perovskite-type ($Li_xLa_yTiO_3$, LLTO), and garnet-type ($Li_7La_3Zr_2O_{12}$, LLZO) materials [31]. All oxide-based electrolytes are stable in ambient air which can simplify large-scale manufacturing and improve safety [12].

Among oxide-based SSEs, NASICON-type electrolytes have the highest ionic conductivity (>1 mS cm^{-1}), wide potential windows, and good chemical stability [32]. However, they are chemically unstable towards the Li metal anode. To enhance electrochemical stability and extend cycle life, a protective interlayer (<5 µm) would have to be applied between the anode and the electrolyte [33,34]. Perovskite LLTO exhibit high ionic conductivity (1 mS cm^{-1}) but is not stable against Li [35]. However, efforts are being made to enhance its electrochemical stability by ionic doping, a common method used to stabilise the crystal structure [36]. Garnet-type electrolytes have ionic conductivities ranging from 0.1 to 1 mS cm^{-1} and are electrochemically stable against Li metal [35,37,38].

All sulphide-based electrolytes are classified as glassy or glass-ceramic materials and can be further divided into 3 groups, namely, lithium thiophosphates or LPS (Li_2S-xP_2S_5 system), argyrodite type (Li_6PS_5X; X: Cl, Br, I), and LGPS ($Li_xMP_xS_x$, M: Sn, Si, Al, Ge) [39,40].

Lithium thiophosphates are investigated due to their good electrochemical stability, ductility, and low cost, but depending on the composition, ionic conductivities of 75Li_2S·25P_2S_5 and $Li_7P_3S_{11}$ are equal to 0.2 and 17 mS cm^{-1} respectively [41,42].

$Li_{10}GeP_2S_{12}$ (LGPS) shows remarkably high ionic conductivity (>10 mS cm^{-1}) [43]. Among argyrodites, the chlorine-rich argyrodite has a high ionic conductivity of 1 mS cm^{-1} much higher than the bromine-rich and iodine-rich ones, which have much lower ionic conductivities in the range of 10^{-6}-10^{-4} S cm^{-1} [44].

The ionic conductivities of sulphide electrolytes are higher compared to those of oxide electrolytes. However, oxides are more electrochemically and mechanically stable relative to sulphides and polymers.

Glassy solid-state electrolytes (GSEs) are considered a distinct subclass of inorganic SSEs. These materials include oxysulphide, oxynitride, and mixed oxysulphide-nitride glasses, which exhibit good electrochemical stability against Li metal anode [45–49].

Glassy oxynitride GSEs, such as lithium phosphorus oxynitride ($Li_xPO_yN_z$, LiPON), are a classic example of an SSE that is mechanically stable and resistant to lithium dendrites [50]. LIPON forms a thermodynamically stable interphase when paired with a metallic lithium anode yet exhibits low ionic conductivity of 10^{-7}~10^{-6} S cm^{-1} [51,52]. Currently, the deposition of amorphous LiPON is limited to physical vapour deposition (PVD) methods such as RF magnetron sputtering, therefore its use in a large-format pouch cell is technically infeasible [53]. The market potential and scalability are low and LiPON electrolytes are currently only used in solid-state micro-batteries used for small devices [54].

In the case of oxysulphide GSEs, binary systems such as sulphide LPS in which P_2S_5 is substituted with P_2O_5 or B_2O_3, are used to prepare mixed-glass former (MGF) systems using melt-quenching technique [55]. Some of the glasses containing P_2O_5 exhibited ionic conductivities as high as 3 mS cm^{-1} [56]. Grain boundary-free ionically conductive oxysulphide and oxynitride SSEs can be formed in homogeneous and continuous glass forms by casting and drawing [57,58].

Hybrid solid electrolytes (HSE) are composite materials, which have attracted attention as they combine SPEs and SSEs [59]. In this concept, the active inorganic fillers participating in ionic conductivity are encapsulated in polymers that are electrochemical compatible with the Li metal anode.

3 Solid-state electrolyte (SSE) challenges

3.1 Interface challenges

In a cell, the SSE is in contact with both the cathode and anode. Excellent contact is required, as poor contact between the SSE and electrodes will result in poor interface performance, and ionic conductivity [60]. In general, there are two categories of reactions that affect interfaces in SSEs. The chemical reactions that occur during the storage and fabrication process of the cell, and electrochemical reactions that occur on the electrolyte interfaces while the cell is operating under applied potentials (charging/discharging) [61]. Additionally, the chemical instability of the electrolyte materials at their interface, due to their reaction with ambient air, may limit their applications for high-energy density SSBs [13]. All interface challenges are briefly discussed below.

3.1.1 Li anode-SSE interface

Among the diverse spectrum of SSEs, the garnet-type LLZO-based electrolytes are considered the most appealing candidates on account of high ionic conductivity, excellent chemical/electrochemical stability [62–65] and potentially high energy density with good stability against the metallic Li anode [66,67]. However, various challenges limit the application of all SSE materials, mostly due to interface issues.

Most SSEs are reduced upon contact with Li, leading to high interfacial charge transfer impedance and accelerating dendrite formation [68]. In the case of chemically stable interfaces (Li/LLZO, Li/Li_3PS_4), a significant failure mechanism has been attributed to the growth of lithium dendrites from inhomogeneous current density distribution [13]. Due to the rigidity of the garnet-based electrolytes, forming good contact between the garnet and metallic Li is

challenging, resulting in high resistance in the interface, thereby limiting the performance of SSBs.

Perovskite-based materials (such as LLTO), have higher ionic conductivity compared to conventional electrolytes at room temperature [69]. However, upon contact with Li anode, Ti^{+4} is reduced to Ti^{+3} and increases the electronic conductivity due to the presence of mixed Ti^{+3} and Ti^{+4} ions [70]. The formation of an unstable layer at the Li/electrolyte interface can hinder lithium dendrite propagation. However, Li^{+} ion transport is also inhibited, increasing cell impedance, and limiting the cell lifetime [71,72].

Another issue with using a Li anode is the 100% volume change of Li metal during charge/discharge, requiring an excess Li metal supply of 20%-300% [73]. This decrease in the volumetric energy density initiates stresses, shape change, destabilises interfaces, and reduces cycle life. Volume changes can lead to pressure fluctuations, where localised stresses at the interfaces (Li/SSE) may result in mechanical failures in the solid electrolyte, such as cracking, bending, loss of contact, and low coulombic efficiency during cycling [74].

Sulphide-based electrolytes have high lithium-ion conductivity, but their electrochemical windows are narrow [75]. At the Li anode, a solid electrolyte interphase (SEI) is formed that contains decomposed products, such as Li_2S, Li_3P, or LiCl. Due to the notably lower ionic conductivity of the decomposed products, interface resistance increases, leading to deterioration of the battery performance [76]. Sulphide-based electrolytes react with Li metal, restricting the use of Li metal at the anode [77]. Currently, using non-lithium metal anode materials such as silicon or graphite is the only viable option due to electrochemical stability [78].

In summary, progressive deterioration of the Li/SSE interface can occur in most systems; through the high chemical reactivity between Li metal anode and solid electrolytes, including LATP, LAGP, and LGPS; poor solid-solid contact between Li metal and a solid electrolyte, such as LLZO; or considerable volume changes during Li discharge and charge. Securing good contact between interfaces, enhancing the interface kinetics, and maintaining morphological stability between Li/electrolyte interface is extremely difficult during cycling [79].

Based on the classification proposed for the first time in 2015 [80], the interfaces between metallic Li and SSEs are classified into 3 groups according to their electronic and ionic conductivity (Figure 2): (1) Thermodynamically stable interfaces, where no reaction with Li occurs (Li/LLZO, Li/LLTO); (2) Mixed conducting interfaces, in which ions and electrons can transport simultaneously (Li/LATP, Li/LAGP); (3) Ionically conductive but electronically

insulating interfaces, where electrolytes hinder direct reaction but allow Li-ion conduction (Li/β-Li_3PS_4). It is worth noting that dendrite formation between Li metal and LLZO, widely reported in Group 1, is less observed in the other two groups [81,82].

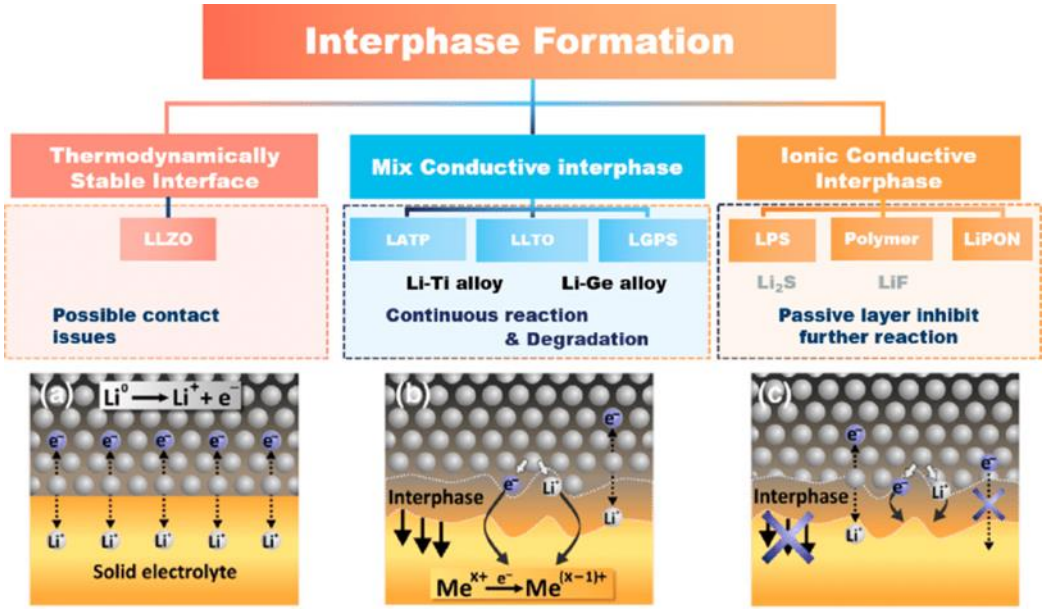

Figure 2. Illustration of three types of interphases between SSE and metallic lithium. Adapted from [13].

3.1.2 SSE-cathode interface

Among various solid electrolytes, oxide-based solid electrolytes are considered safe and chemically stable due to their neutrality or lower reactivity with ambient air [60]. However, garnet-type cubic LLZO electrolytes are reported to be unstable with the cathode materials such as lithium cobalt oxides (LCO), lithium nickel manganese cobalt oxides (NMC), and lithium nickel cobalt aluminium oxides (NCA) when heated to high temperature during the cell fabrication process [83]. Among these three cathode materials, LCO shows optimal chemical stability with LLZO as a solid electrolyte.

The poor chemical stability of glassy sulphide-based electrolytes is ascribed to their structure, chemical bonding, and nonbridging sulphur (NBS) units in the glassy network [77]. Poor chemical stability, such as oxidation from spontaneous chemical reactions, was observed for Li_3PS_4 electrolyte when using NMC and NCA as cathode materials [84,85].

Alongside chemical stability, good electrochemical stability of solid electrolytes is an additional major factor for commercial adaption. The electrochemical stability window refers to the stability of the bulk material, rather than a specific interface with an active material. However,

the electrochemical decomposition of solid electrolytes typically takes place at the interface once they experience a potential beyond their oxidation limit or electrochemical window [86].

In oxide-based electrolytes, the co-sintering process is used to improve the contact, due to the solid and rigid interface between the oxide electrolyte and cathode particles. However, this results in new interphases and further complicates the interfacial behaviour [87,88]. The interfaces that are formed by mutual diffusion during the thermal process result in high interfacial resistance [89].

The type of cathodes can affect the electrochemical performance and interfacial behaviours [13] due to the formation of various electrochemically decomposed products with different ionic and electronic transport properties. Once conductive interfaces are formed, continuous interfacial reactions may occur. LCO cathode in conjunction with oxide perovskite electrolytes displays 6 times higher interfacial resistance than the $LiMn_2O_4$/oxide perovskite interface [90].

Another reason for the high interfacial resistance and instability of the solid electrolytes and cathodes in ASSBs is the formation of a space charge and interdiffusion layer at the interface between the cathode and solid electrolyte. A significant voltage drop of the LCO/NASICON interface observed during cell cycling was attributed to the formation of a lithium depletion zone [91]. LMO and LFP cathode materials strongly react with garnet-based electrolytes under high potential, but LCO is stable [13]. So far, LCO has been demonstrated to form more stable interfaces with LLZO than other active materials, with in-depth studies on the interfacial impedance and performance of a full cell with LLZO-LCO cathode composite [86].

The poor performance of the SSBs based on oxide electrolytes is correlated with several factors: (1) High polarisation resulting from the poor contact between SSEs and cathode materials; (2) High electrical resistance of the layer formed during thermal processing; (3) An interphase layer resulting from electrochemical decomposition at high voltage; (4) The space charge layer effect; while the Li^+ can move in SSEs while the host ions are constrained within their original sites, a Li depletion zone is formed and limits lithium movement in subsequent discharge processes.

Sulphide-based electrolytes are soft materials and therefore they can form a conformal contact at their interface with the cathode [92]. Unlike oxide-based electrolytes, sulphide electrolytes have narrow electrochemical stability, and there are considerable differences between the various sulphide material sub-classes. In addition, sulphides are prone to reaction at low potentials with lithium metal anode and at higher potentials with the cathode materials [30]. Like oxide-based electrolytes, in sulphide electrolytes, the space charge layer forms that may

negatively affect the cathode and electrolyte interfaces, especially, when sulphide-based electrolytes and high-voltage oxide cathode are involved [92].

3.2 Fabrication challenges of SSEs films

In a conventional lithium-ion battery, the typical separator thickness used with liquid electrolytes is 25 μm [93]. When utilising a solid electrolyte, reducing thickness becomes essential, leading to decreased resistance, improved ionic conductivity, and positive effects on general cell performance [13,60,94,95].

For glass-ceramic and ceramic materials, the most straightforward bulk-forming method involves preparing a pellet by cold pressing [96]. However, pressing powder in a die is typically suitable only at a laboratory scale and is insufficient for producing the thin samples required for mass production. Considering the continuous nature of thin film fabrication, batch-type processes (forming or sintering) might not be suitable for commercial manufacturing. Identification of challenges and resolving issues associated with forming, densification, and sintering methods are crucial for achieving a fully dense monolithic material. The current primary processing challenge involves transitioning from pellets, which serve as basic model systems, to a continuously homogeneous, dense, crack-free, and phase-pure film [11].

Stability is another challenge in solid-state electrolyte processing, defined as the ability to maintain morphology, composition, and structure after being exposed to other battery constituents. Most stability concerns, including chemical, electrochemical, mechanical, and thermal, have been previously reviewed [13]. Chemical stability remains a significant challenge for oxide- and sulphide-based materials, especially in the context of green body forming. Thin film processing and scalable electrode manufacturing will require the use of dry/wet processes in conjunction with binders and other inorganic or organic additives.

Most sulphide-based electrolytes pose safety concerns and must be handled with care because these materials are sensitive to humid air and can react with moisture to produce poisonous H_2S gas [94]. Consequently, all forming and processing must take place under an inert gas atmosphere (<5 ppm O_2). Some oxides such as Fe_2O_3, ZnO, and Bi_2O_3 and lithium halide additives have been shown to potentially improve the chemical and electrochemical stability of sulphide SSEs and partially suppress the generation of H_2S in humid air [94,97].

3.2.1 Solvent-based systems

Commercial Li-ion battery electrodes are manufactured using a slurry casting process in a roll-to-roll manufacturing method. The slurry, containing active material, conductive carbon, and

binder in a solvent, is cast onto a metallic current collector. Typically, a toxic N-methyl-2-pyrrolidone (NMP) solvent [98], is uniformly mixed with a polyvinylidene fluoride (PVDF) binder, a conductive agent, and the active material [99].

From a ceramic perspective, the binders used for conventional lithium batteries are not those typically considered for ceramic body forming. Green body formation requires inert binders, which provide strength by bridging the particles. Complete absence of binder is undesirable as there would be no soft matrix to buffer the expansion and contraction of rigid crystalline particles of the active material. After green forming, a debinding step is conducted at a controlled heating rate to remove the organic binder. The formed brown body is then sintered (at 80-90% of melting temperature) to consolidate the material without melting the particles, achieving the final dense microstructure. Additional post-processing steps such as machining, grinding, and polishing can be carried out to ensure the parts have the desired surface finish and comply with required tolerances.

The use of more environmentally friendly binders, which decompose thermally into residual ash and release non-toxic gases, is desired. Several alternatives to fluoropolymers that are ethanol processable and fluorine-free have been identified [100]. Binders such as polyacrylates, aliphatic polymers and oligo- and polysaccharides are commonly used in ceramic forming and processing. Depending on the sintering atmosphere choice, various systems can be implemented. During firing, the binder can be removed through vaporisation to avoid combustion of the polymeric binder, resulting in an ash-free and water-free system [101].

Both oxide- and sulphide-based electrolytes suffer from a nucleophilic attack of polar functional groups of aqueous and polar organic solvents, limiting their processing to less polar or preferably non-polar options [97]. Al-LLZO was treated with various solvents; Li leaching was high for primary alcohols (MeOH, EtOH, n-PrOH) and less pronounced for the nonpolar organic solvents (i-PrOH, AcN, c-Hex) [102]. Irreversible Li-ion loss due to a Li^+/H^+ cation exchange process is well-known for LLZO upon solvent immersion. The use of nonpolar solvents aided in preserving the crystal structure. A similar study was also conducted on Ta-LLZO [103] where several common organic solvents with typical functional groups were tested. Li leaching and lattice swelling occurred in all solvents; however, the electrolyte was much more stable in weaker acidic compounds such as 1,3-dioxane and n-hexane.

A solvent compatibility trial towards sulphide SSE ($Li_7P_3S_{11}$) was reported [104] with 9 common solvents (such as MEK, THF, NMP, DMF) to examine the stability of an LPS electrolyte.

Chemical degradation was observed in most cases as the electrolyte is extremely reactive with polar solvents such as N-methyl-2-pyrrolidinone (NMP). Crystalline properties were retained only by using nonpolar toluene (TOL) and p-xylene (XYL). Sulphide SSEs have outstanding processability due to their softer nature. However, poor chemical stability towards solvents and binders may significantly limit their large-scale manufacturing compared to oxide SSEs [105].

3.2.2 Aqueous-based systems

In wet processing methods, aqueous processing offers several advantages over the use of organic solvents. Water is a green solvent, with low-cost and health and safety risks as it is non-toxic and non-flammable. It is believed that less expensive and environmentally friendly solvents, including water, could eliminate the large capital cost associated with solvent recovery systems for most solvents [106]. However, aqueous processing also has disadvantages due to extended drying times, low tolerance to changes (pH, temperature) and limitation in binder choice.

Upon contact with water, the surface of active material particles is altered, notably by the formation of LiOH and Li_2CO_3 species, which deteriorate the reversible capacity and cycle performance [107]. Garnet solid electrolytes which are stable in air, have been found to form a passive surface layer in contact with humid air. This not only poses challenges during processing but impairs the battery performance. It was reported that polar solvents in a slurry-based wet-processing of the LLZO, for example, tape-casting, result in irreversible Li-ion loss of the pristine material [102]. This instability against moisture is attributed to the Li^+/H^+ exchange reaction between the material and water [17]. Because of the low stability of electrolytes in water, aqueous-based compositions are not recommended for SSE manufacturing.

3.2.3 Lithium loss mitigation strategies in oxide SSEs

Scalable manufacturing of SSEs is prevented by the effort required to maintain the necessary high lithium content. Once a green body is formed, solid electrolytes, particularly oxide-based materials such as LLZO and LATP, can be formed and sintered similarly to traditional oxide ceramics. However, due to the volatility of lithium, maintaining the correct stoichiometry is challenging with typical high-temperature processes. Faster and lower temperature sintering processes are suggested to reduce processing costs and volatilisation, and to increase energy efficiency. Maintaining high density and conductivity can be achieved through mitigation strategies which include lowering the sintering temperature and time [106].

Li loss from the system impedes densification [108]. Common methods to reduce Li loss includes enclosing the material in sealed crucibles, burying the green part in a parent powder [108–110], doping pellets with additional lithium [111] or a lithium-containing sintering aid [108,112]. Since covering with a sacrificial parent powder is not expected to be a viable solution at the large manufacturing scale, other options must be explored. Due to the costs of using additional sources of volatile ions and the difficulty of industrial scaling of such a process, an alternative approach of reducing the sintering temperature and duration is suggested, offering additional efficiency benefits for large-scale manufacturing.

Sintering aids are inorganic lithium-ion conductors used in liquid-phase sintering. These materials undergo sintering with the electrochemically active material to yield fused particles in a sintered material. Sintering aids maintain liquid phases at high temperatures, reducing the crystallisation temperature and enhancing the densification of ceramics to some extent. Liquid-phase sintering is a viable technique to improve the density of sintered electrolytes [113]. Commonly used sintering aids with a low melting point are oxides such as ZnO, MgO, and B_2O_3 [114] or lithium salts such as Li_2O, Li_3PO_4, Li_3BO_3 [115], $LiBO_2$ or LIF [116–118].

Sintering aids form a glass-like phase at grain boundaries to improve contact between grains and lower the grain-boundary resistance. Al-LLZO sintered with the addition of MgO (0-7 wt.%) as a sintering aid resulted in sheets with densities of up to ~91% [119]. The formation of an Al_2O_3-Li_2O eutectic was suggested to enhance the sintering rate of Al-LLZO at the temperature of 1055°C [120]. In another case, Al-LLZO was sintered with 1 wt.% of sintering aids such as Li_3BO_3, Li_3PO_4 and Li_4SiO_4 at 900°C for 36 h or 1200°C for 12 h, with a sacrificial parent powder, the highest theoretical density of 96% and ionic conductivity achieved for pellets sintered at 1200°C using Li_4SiO_4 [112]. The addition of sintering aids appears to improve density, structural integrity, and ionic conductivity.

Compatibility of Li_3BO_3 with LLZO and Nb-LLZO was confirmed with dilatometric analysis which showed the onset of sintering as low as 710ºC [115]. $LiBO_2$ and Li_3BO_3 aids were used to enhance the density of LLZO and structures with larger grain size and enhanced electrical conductivity at 900°C sintering temperature [121]. In general, the action mechanisms of sintering aids are reflected in increasing density and promoting Li^+ transport at grain boundaries. The addition of sintering aids appears to improve the density, structural integrity, and ionic conductivity.

4 Processing of Solid-State Electrolytes

4.1 Forming

The forming step is the physical process whereby the ceramic material is transformed from a suspension or powder paste to a green (unsintered) body. In the case of crystalline materials, such as oxide SSEs, the green density is crucial and determines the amount of shrinkage required to densify a ceramic body. Higher powder packing density leads to higher density after sintering.

Oxide-based polycrystalline SSEs require high-temperature (>600°C) sintering to improve the particle-particle contact, enhancing ionic conductivity. These materials can be treated as any other oxide (ceramic) and can be formed into a green body and sintered through various methods. Among all SSE compositions, the garnet-based Ta-, Ga-, Al-doped LLZO and LATP electrolytes have been most studied [95].

Glassy and glass-ceramic materials have low grain boundary resistance and can be processed at lower temperatures compared to crystalline oxide SSEs. The formability of sulphide systems may result in improved interfacial contact [42,122] by using pressure and temperature to create low-impedance interfaces with electrode materials [123]. Instead of using melt-quenching method, mechanochemical milling (MCM) can be used to produce glasses without the evaporation of the active material [124]. MCM glasses are typically milled at high speeds for prolonged periods to achieve the loss of crystalline structure in the material [125,126]. The resulting powder can be used in all common ceramic forming methods such as tape casting or hot pressing.

While oxide SSEs are stable in air, sulphide SSEs are prone to reaction with moisture to produce toxic H_2S gas, limiting their immediate scalability [127]. Due to the poor chemical stability of sulphide SSEs, a dry inert gas atmosphere is required for all processing steps to maintain safety standards [128,129]. The necessity of using an argon-filled glovebox increases the cost. Safety risks exist even post-processing, as accidental battery damage can lead to H_2S and SO_2 formation [130].

4.1.1 Thin film deposition techniques

Currently, thin film SSEs fabricated with amorphous LiPON, or LiPON-derivatives (lithium phosphorus oxynitride) are used in commercially available rechargeable micro-batteries such as implantable medicine and smart devices [54] and are produced by companies such as Cymbet [131], Ilika [132] and Excellatron [53]. However, the use of thin film deposition

technologies is currently limited to small-scale applications due to the high investment costs of vacuum deposition processes such as RF magnetron sputtering [53,133].

High-quality dense self-standing LLZO thin films have been successfully fabricated using pulsed laser deposition (PLD) [134–136], chemical vapour deposition (CVD) [137], metal-organic vapour deposition (MOCVD) [137], atomic layer deposition (ALD) [138], magnetron sputtering [139,140], and sol-gel deposition [141,142]. These methods enable the homogeneous growth of thin films (0.2-1 µm) over large areas with high deposition rates and high purity [143]. Although methods such as magnetron sputtering and PLD can result in a high-density LLZO film, Li loss during deposition remains a challenge and a non-conductive pyrochlore phase ($La_2Zr_2O_7$) tends to form in lithium-deficient films upon crystallisation.

Physical vapour deposition (PVD) methods such as pulse laser deposition (PLD) have been used extensively to prepare sulphide-based thin SSEs. However, the atmosphere in which sulphide materials are processed requires special consideration due to the extreme sensitivity of the compounds to ambient moisture content [144]. A 50–70 nm thin $80Li_2S{\cdot}20P_2S_5$ solid electrolyte (SE) films were successfully coated on an LCO cathode under an argon atmosphere [145].

The reported films vary from dense and crack-free to highly porous structures. In the case of sol-gel deposition, outgassing organics from the films can cause pores and cracks [136]. Despite much-conducted research, detailed parameter studies are still missing in the field of SSE thin film processing. Most successful depositions have been demonstrated only at a laboratory scale; but all thin film deposition methods consist of complicated multiple steps, which are expensive and time-consuming, making them unsuitable for large-scale SSEs manufacturing.

4.1.2 Tape Casting

Tape-casting has emerged as a promising candidate for the scalable and low-cost commercial fabrication of SSE layers because this technique is not limited to the preparation of single-layer ceramic SSEs. Repeating casting steps or using roll-to-roll processes can lead to multi-layered, co-sintered materials [30]. In this method, ceramic powder is mixed into a slurry with addition of a solvent, an organic binder, and often a plasticiser to improve the green strength. The slurry is then spread into thin sections using an automated doctor blade coater.

Conventionally tape cast-sintering of 22-25 µm thick and dense (94-95%) Al- and Ga-LLZO flexible films resulted in ambient ionic conductivities as high as 1.3 mS cm^{-1} [146,147]. The packing density of dried green films (~45 µm thickness) was improved by thermo-compressing

under nitrogen before sintering. Al-LLZO films can also be tape-cast and sintered in ambient air [148]. Cross-sectional SEM micrographs of the Al-LLZO air-sintered films (Figure 3) showed nanosized pores formed between primary Al-LLZO particles.

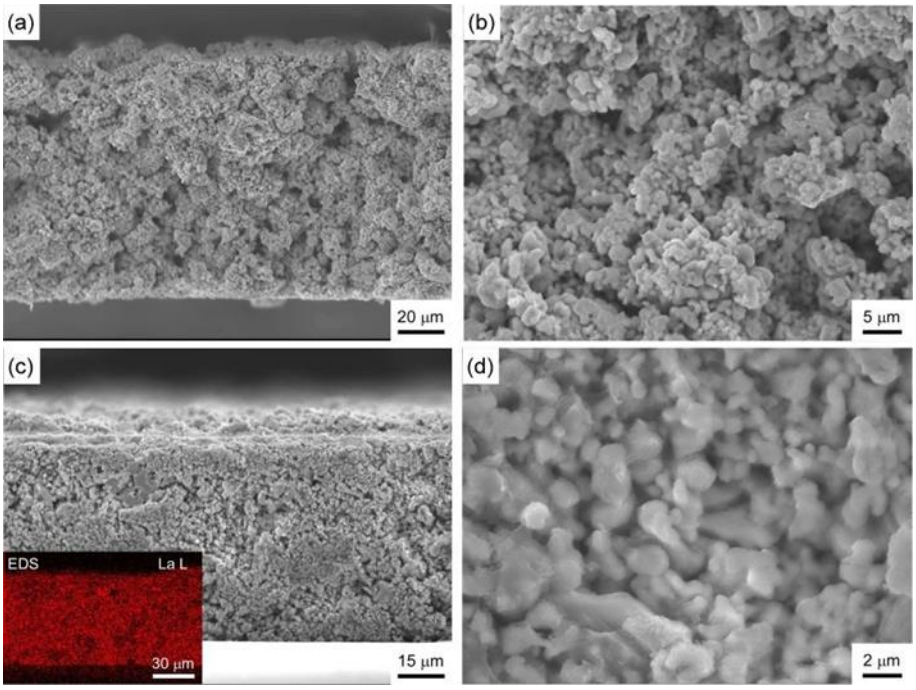

Figure 3. SEM micrographs of the as-cast and cold-pressed Al-LLZO sheet electrolytes. (a) Cross section of the as-cast sheet electrolyte, (b) enlarged view of part of the cross-section shown in (a), (c) cross-section of a 150 MPa cold-pressed sheet (inset: EDS mapping of La), and (d) enlarged view of part of the cross-section shown in (c). Adapted from [148].

A summary of SSEs prepared by tape casting is presented in Table 1. Factors to be considered in the satisfactory preparation of green tape cast sheets include: (1) slurry viscosity controlled by the ratio of the components (powders, binder, plasticizer, dispersant, solvent); (2) drying and debinding conditions to obtain flat and homogeneous tape; (3) choice of sintering temperature and time for final tape densification. In the case of oxide SSEs, the choice of solvent and binder did not have a considerable effect on the final properties of the sintered electrolyte, and the properties of green tapes should not be used as a proxy for the quality of the final sintered part [119]. Considering the final part must be debinded followed by sintering, attention should also be paid to the sintering atmosphere.

Wet processing of sulphide SSEs is complex due to difficulties in finding matched pairs of sulphide SSEs, solvents, and polymeric binders [149]. Highly reactive sulphide SSEs decompose in contact with solvents that are commonly used in tape-casting; these include water and other organic solvents with a polarity index >4.0 [150]. This limitation narrows down

the selection of binders that need to be soluble in the solvent, inert in contact with the SSE, and capable of maintaining the ionic conductivities of SSE as much as possible [105].

Examples of tape-cast Li-ion conducting HSEs also include films fabricated using sulphides as active material. Encapsulated in various polymers (PEO, PVDF, NBR, SEBS), $Li_7P_3S_{11}$ powder was tape cast using xylene as a solvent [104]. Thick films (~50 μm) displaying high room temperature conductivity (0.7 mS cm^{-1}) and good stability with a Li metal anode were prepared. Defect-free LPSCl films of 50 μm thickness were prepared using ~5 wt.% of NBR binder in a mixture of toluene and isobutyl isobutyrate as a solvent [150]. The binder did not negatively affect the ionic conductivity (~1.12 mS cm^{-1}) of the film as the properties were comparable to a cold-pressed, binder-free, thick LPSCl pellet (~1.10 mS cm^{-1}).

Table 1 Examples of fabrication of oxide-based SSEs by tape casting.

Active material	Dispersant	Binder	Plasticizer	Solvent	Sintering aid	Sintering conditions	Thickness (μm)	Sintered Density (%)	Ref.
Al-Ta-LLZO	BYK 180	PVB98	PEG400	Ethanol Butanone	-	1175^{0}C 10 h, air	50-240	92.8	[111]
LLZTO	-	Polyacrylic resin	Methyl benzoate	Ethanol Butyl acetate	1.2 wt.% Li_2O	1100^{0}C 6 h, air, sacrificial powder	~200	~99	[151]
Al-LLZO	-	PVB98	Benzyl-butyl phthalate (BBP)	Ethanol Acetone	-	1090^{0}C 1.5 h, Ar	25-55	~95	[152]
Al-LLZO	Dispex Ultra PA 4560	Methylcellulose	PEG300	Water Ethanol	5 wt.% MgO	1115°C 3 h, Ar	~100	91.1	[119]
Al-LLZO	Polyacrylic acid	PVB	Benzyl-butyl phthalate (BBP)	Ethanol Acetone	-	1090°C 1 h, N_2	22	94	[146]
Ga-LLZO	Polyacrylic acid	PVB	Benzyl-butyl phthalate (BBP)	Ethanol Acetone	-	1139°C 0.3 h, N_2	25	95	[147]
LLTO	Triethanolamine	PVB	BBP	Ethanol	-	500^{0}C 2 h, 1050^{0}C 2 h, 1260^{0}C 12 h, air	25	N/A	[153]
LLZNbO	Menhaden oil	Ethylcellulose	PEG400 Dibutyl phthalate	Ethanol Toluene	0.5 wt.% Li_3BO_3	1000C, 6 h, Ar	150–175	90.8	[154]
Al-Ta-LLZO	-	Methylcellulose	PEG, Glycerol	Water	-	1175°C 4 h, air	~150	~90	[106]
LATP	Hallotannin	Polymethyl-methacrylate	PEG4000 Dibutyl phthalate	Acetylacetone Isopropanol	-	1100^{0}C 2 h, air	20	95	[155]
LATP-AP	Menhaden oil	PVB-VA-VAc	BBP PEG	Ethanol Xylene	-	450^{0}C 1h, 1080^{0}C 1h	40	>90	[156]

4.1.3 Screen Printing

In this method, a rubber blade called a squeegee is pulled across the top of the screen covered with a thin mesh. The blade pushes a shear-thinning ink with low viscosity through the mesh onto the surface of the substrate. Screen printing can be easily combined with tape casting for composite preparation, for example, to screen print an additional conductive buffer layer on top of a pre-sintered or raw substrate cast tape [157].

There are examples of cathodes or interlayers being fabricated on top of an SSE by screen-printing through the development of shear-thinning inks. A 10 µm thick cathode layer of LCO and Li_3BO_3 (75:25 wt.%) was screen printed onto a pellet of Nb-LLZO (Figure 4) [158]. The interface between the cathode and electrolyte was improved by annealing the sample at 700°C for 1 h to remove all binders and melt the Li_3BO_3. In another example, an LCO cathode (50 µm) was screen printed on top of a Ta-LLZO sintered pellet (300 µm) [159]. Co-sintering was performed at 1050ºC in air for 30 min and resulted in much lower area resistance during charge and discharge cycling.

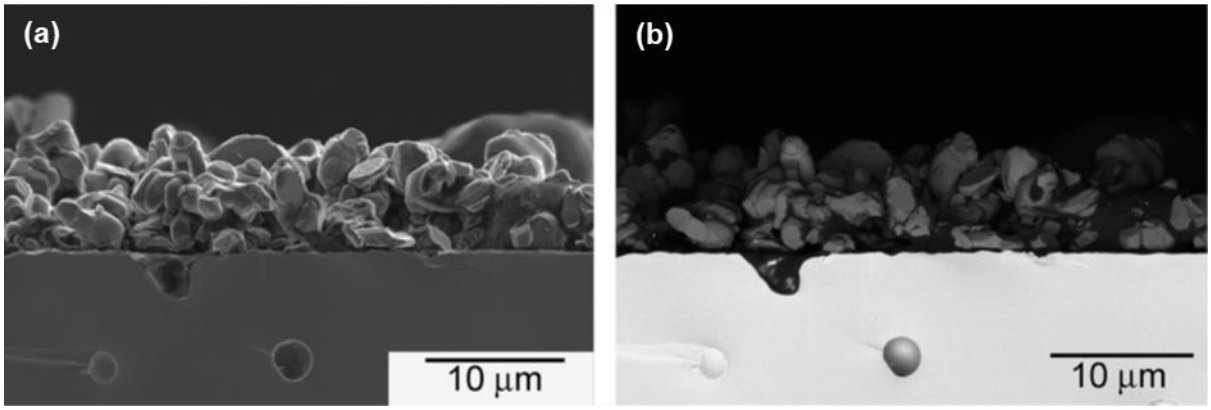

Figure 4. Cross-sectional SEM images of (a) secondary electron and (b) backscattering electron images of the interface between the positive electrode layer and the Nb-LLZO solid electrolyte[158] .

In the case of interlayers, a thin (10 µm) phase transition layer was fabricated by screen printing on the interface between LLZO-$0.3B_2O_3$/$LiMn_2O_4$ (LMO) [38]. The layer was a mix of 50:50 (wt.%) $LiMn_2O_4$ and LLZO-$0.3B_2O_3$ powder with ethyl cellulose as a binder. Grain boundary resistance was reduced at the interlayer by annealing the sample at 700°C for 1 h.

To address issues with lithium dendrite formation and poor interfacial wetting between the Li-metal anode and the solid electrolyte an amorphous Li_3BO_3 (LBO) glassy interlayer (~5 µm) was screen printed onto an LLZTO pellet and annealed at 725 °C for 1 h [160]. Interfacial conductivity increased by 10 times and the cell showed no sign of severe defects, confirming the positive role of the LBO interlayer in preventing the Li-dendrite penetration.

4.1.4 Electrophoretic Deposition

In electrophoretic deposition (EPD) method, the material is dispersed into a suspension, typically an organic solvent. An electric field is then applied to force the deposition of the powder onto an oppositely charged conductive substrate. Electrophoretic deposition (EPD) is a method with a high TRL and has been demonstrated in industrial operations to manufacture beta alumina (Na-β″-Al_2O_3) electrolytes for sodium-sulphur cells and surface coatings in automotive industry [161].

A composite separator (25 µm thick) was manufactured through the co-deposition of LLZTO particles with a PVDF-HFP colloid using an applied field of 72 V [162]. Additionally, there is an example of LPS thin films (10-100 µm thick) produced from LPS precursor (Li_2S-P_2S_5) dissolved in a non-polar dehydrated ethyl propionate (EP), followed by warm pressing at 220°C [163].

4.1.5 Aerosol Deposition

In this technique, a carrier gas accelerates and transports micrometre-sized powders, which are directly sprayed onto the surface intended for coating. The process does not require binders or solvents to prepare uniform dense films ranging from 1-100 µm in thickness. Aerosol deposition is a low-cost manufacturing method that operates at ambient temperature. However, the process necessitates the use of a deposition chamber.

Using powder aerosol deposition method, 30 µm thick Al-Ta-LLZO films were prepared on a copper substrate (Figure 5). After deposition, surface roughness was reduced through polishing, eliminating nonconductive Li_2CO_3 residual and ensuring a homogeneous electrical field distribution [164].

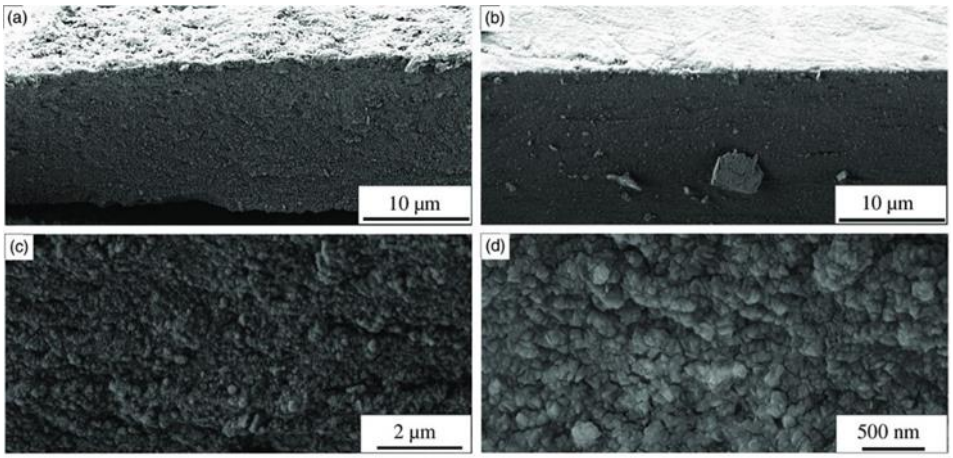

Figure 5. Fractured cross-sectional SEM images of the Al-Ta-LLZO film in (a) the as-deposition state before and (b–d) after polishing. c-d) Higher magnifications validate the dense and nanocrystalline structure of the films [164].

The microstructure and density of the fabricated films are significantly influenced by the size and the morphology of raw powder. Controlling the particle size distribution and employing post-annealing processes can enhance the conductivity of the SSE films [165]. For instance, 20 µm thick Al-LLZO films, prepared by powder aerosol deposition without an annealing process, exhibited limited ionic conductivity, reaching only 10^{-8} S cm^{-1} even at 140°C [166]. However, post annealing of Al-Ta-LLZO films (~10 µm thickness) at 600ºC restored the ionic conductivity to the bulk value [167].

4.1.6 Hot Powder Rolling

Hot powder rolling or dry pressing offers an alternative method for thick film fabrication. In this technique, only electrochemically active components are utilised, eliminating the need for drying and solvent recovery steps, which significantly reduces both cost and time [168]. Because this method involves minimal solvent handling, it can be employed in solvent-free conditions [169,170] or even completely solvent-free and/or binder-free settings [171], making it highly versatile for SSEs manufacturing.

This approach has been successfully applied not only in the fabrication of solvent-free cathodes [172,173] but also in the manufacturing of composite electrolyte membranes (PEO/LLZTO) [174]. For instance, a high ionically conductive sulphide SSE was developed by homogenous mixing of LiPSCl and PTFE (0.2 wt.%) powder and subjecting it to hot calendaring at 80°C, resulting in a flexible film with a thickness of 30 µm [175]. To further enhance performance, an additional magnetron sputtered Al_2O_3 interlayer was introduced at the SSE/Li interface, improving the anodic stability and suppress internal short circuits.

4.1.7 Additive Manufacturing

Additive Manufacturing (AM) may offer significant benefits over conventional forming methods, including the flexibility of digital manufacturing, reduced material waste, and lighter components. It also provided innovative opportunities for manufacturing advanced components without the need for complex tooling, leading to a reduction in both manufacturing costs and process lead time. Currently, various AM technologies are being evaluated for producing ceramic parts. However, selecting the correct process to match the intended end application is a multi-stage procedure. The choice depends on the desired material's properties such as density, surface finish, size, and geometry. In general, the implementation

of AM within the ceramic industries has been slower compared to the metal and polymer AM technologies. Printed ceramic parts face challenges such as low levels of surface quality, resolution, and mechanical properties compared to conventionally produced components [176].

The emerging AM techniques have revolutionized the device manufacturing sector for electrochemical energy storage. They offer advantages over traditional routes, including their ability for repeatable production of the entire device (electrode/electrolyte/current collectors/packaging). This capability reduces costs and improves the quality of the final product. Additionally, the use of AM enables manufacturers to modify the printed geometries and structures, removing the conventional constraints. This flexibility allows them to surpass the energy-power limits of current SSB systems by adjusting the initial characteristics of the resin/slurry, such as viscosity, composition and printing parameters [177].

Multiple LLZO ink formulations were developed for AM of solid electrolyte microstructures with various properties [178]. The formulated inks were categorised into 2 types: the first formulation was designed for conformal printing, possessing rheological properties required for planar battery architectures [179]. The second type of ink was formulated based on a binder system, giving it Bingham plasticity, ideal for printing self-supporting structures with a high aspect ratio. To demonstrate the range of LLZO electrolyte structures attainable and their variation based on the ink rheology, both inks were printed on LLZO substrates in various pattern arrays. Figure 6 illustrates a schematic of the 3D printing process of solid electrolyte structures, enabling the printing of a wide variety of ordered, high surface area structures. The stacked-array pattern creates a higher surface area within the electrolyte to combine with a Li metal electrode compared to traditional planar structures. This results in the reduced interfacial resistance in the full cell. The notable decrease in the full cell resistance due to improved interfacial contact areas can lead to higher energy and power density of a battery with solid electrolyte. This study demonstrated the applicability of traditional ceramic tape casting recipes in AM of solid electrolytes and outlined a roadmap for further advancements in manufacturing of ceramic SSEs [179].

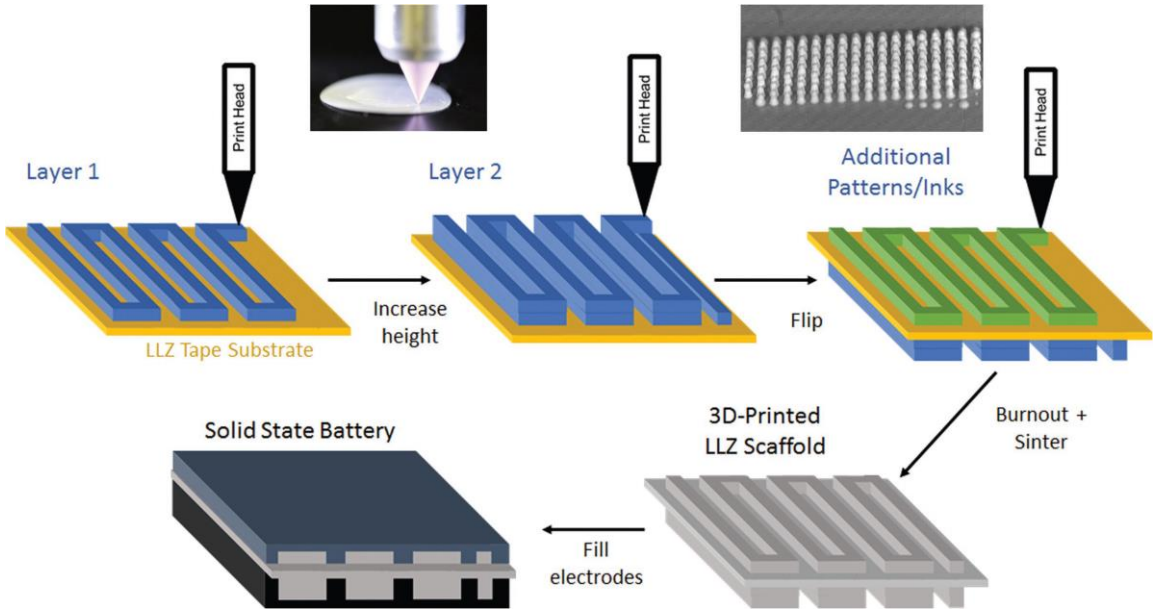

Figure 6 Overview of cell fabrication y using 3D-printing route. Adapted from [178]

Stereolithography (SLA) was emerged as the preferred technique to produce LAGP ceramic electrolytes using glass feedstock [180]. Unlike other AM methods based on light processing, SLA has shown its advantages by overcoming some limitations seen in more commonly used methods like robocasting. Robocasting technique suffers from poor resolution (typically in the order of 100 s of a micrometre) and low-quality surface finishing.

Light-based processing or VAT Photo Polymerisation (VPP) techniques including SLA, Digital Light Processing (DLP), and (Liquid crystal Display (LCD) utilise non-aqueous photosensitive ceramic suspensions, which are formulated with (meth)acrylate or epoxy photo-polymerisable monomers and oligomers alongside other additives such as photo/co-initiator systems [181]. SLA, the oldest among the VPP techniques, employs a laser beam for a point-by-point scanning process to cure the ceramic resin. On the other hand, DLP and LCD, the most recent development, project light in the form of a 2D image to cure the binder plane-by-plane [182].

The ionic conductivity of SLA-printed electrolytes was found to be in good agreement with LAGP fabricated by conventional techniques (6.42×10^{-5} S cm^{-2}) [180]. In the subsequent step (Figure 7), corrugated membranes with a 15% increased interfacial area were printed using the LAGP-formulated resin. These membranes exhibited an equivalent reduction in the area-specific resistance. Moreover, symmetrical cells with lithium metal electrodes were employed to investigate the stripping and plating behaviour of the printed coated electrolytes. The cells showed stable cycling performance over 250 hours, demonstrating the stability of the designed cells.

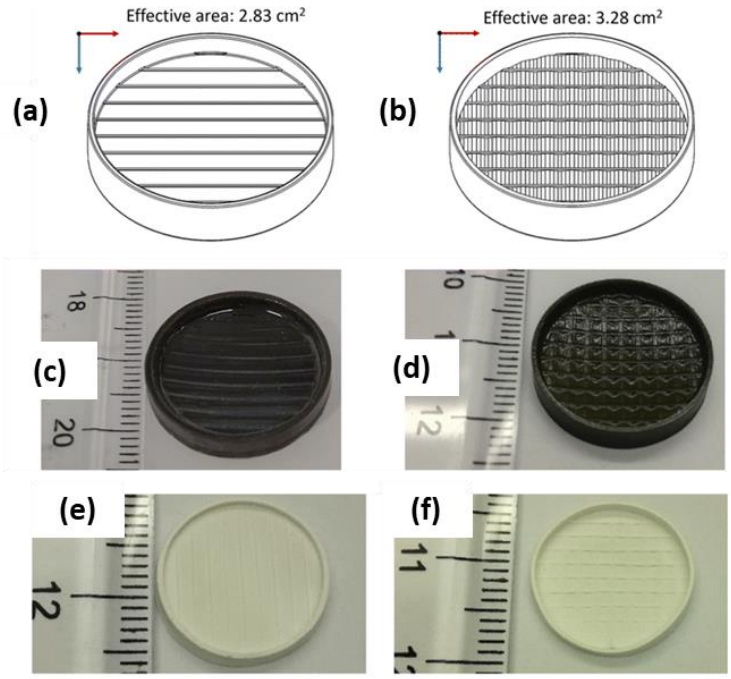

Figure 7 Reference and corrugated LAGP parts - (a) and (b): 3D CAD drawings, (c) and (d): as-printed and (e) and (f): after debinding and sintering. Adapted from [180].

Polymer/ceramic composite electrolytes, comprising ionically conducting or insulating ceramics within polymer matrices, are currently key areas of interest in the SSBs industry. These composites have long been explored as a means to enhance both polymer conductivity and the mechanical properties of the SSEs. The highest values for conductivity in these studies were achieved when nano-sized ceramic powder was utilised, enabling AM technologies to print polymer/ceramic composite effectively [183].

Negative Ceramic AM represents another manufacturing approach involving AM sacrificial polymer moulds that are impregnated with a ceramic slurry by investment gel casting [184] or investment casting [185]. In the following step, the polymer moulds are subsequently removed through a procedure involving either heating or dissolution. The resulting scaffolds are then filled with an inert polymer to enhance their mechanical strength [186]. The main advantage of these methods is the use of polymer AM, which is often more accessible and cost-effective compared to direct additive manufacturing of ceramics. Additionally, these polymer moulds can be manufactured using various AM technologies, such as Stereolithography (SLA) [187,188], Fused Deposition Modelling (FDM) [185,189,190] or Material Jetting (MJ) [191,192].

In a recent collaboration involving Lucideon, KWSP, and Loughborough University, two complementary technologies of AM and contactless Field Enhanced Sintering (c-Flash) have

been investigated for manufacturing textured and specially designed solid electrolyte films for both Li-ion and Na-ion batteries [193]. This innovative manufacturing approach can address technological challenges, including those related to solid-state batteries, thin film processing, improving electrolyte/electrode interfacial area and reducing ion volatilisation. This project also aimed to enhance resources and energy efficiency by exploring the potential combination of two novel and highly efficient technologies, exploiting the strengths of both systems.

4.2 Sintering

Oxide-based crystalline SSEs can be sintered using traditional techniques, typically in a conventional furnace or kiln. In this process, samples are heated by convection and/or radiation techniques in furnaces. Sintering is a crucial step for crystalline electrolyte materials as it enhances mechanical strength, reduces porosity, and lowers grain boundary resistance, consequently improving ionic conductivity. However, optimising the sintering conditions poses a significant challenge in the development of crystalline SSEs.

4.2.1 Conventional Sintering

Conventional sintering methods can draw on centuries of experience with large-scale batch-based or continuous furnaces used in the traditional and technical ceramics industries. Options exist for combining furnaces with different sintering atmospheres, from vacuum to reducing. Options even exist in the marketplace for combining a controlled atmosphere with continuous manufacturing using sequential airlocks. The sintering rate, densification and any initial binder burnout are controlled through the furnace temperature profile.

For oxide ceramics, the sintering temperature is typically over 1000°C, coupled with conventional heating rates of 1-20°C min^{-1}. This results in a slow and energy-intensive sintering process. Samples typically require dwelling at the sintering temperature for a significant period of time (several hours, up to days) to produce parts near the full theoretical density [194].

For electrolyte materials, the volatility of charge carriers such as lithium results in significant loss of the elements over the sintering duration, this changes the electrolyte's stoichiometry and produces phase impurities which reduce the electrolyte ionic conductivity and performance [108]. Doping with an excess of volatile elements or using other mitigation strategies can reduce the material degradation issues but such methods add expenses to a cost-sensitive process. Attempts are made to develop faster or lower temperature methods for sintering ceramics, in the case of electrolytes, these methods are also beneficial by reducing the loss of volatile ions.

Conventional sintering conditions (1100-1220°C for 10-20 h) were investigated to understand the relationship between grain size, density, lithium content and ionic conductivity of Al-LLZO pellets [109]. It was concluded that a combination of high lithium content and densification is required for high ionic conductivity.

An investigation into LLZO powder processing and pellet sintering optimisation has found that small particle sizes (<2 μm) were key to enhancing densification, allowing the use of short sintering time at high-temperatures to reach high densification (~96%) while minimising lithium loss [108].

4.2.2 Hot Pressing

Hot pressing simultaneously applies uniaxial pressure and heating. Uniaxial pressure is applied by driven punches, with an enclosing die heated either through surrounding heating elements or inductive heating of the die itself. The method can rapidly consolidate and sinter powders into dense monoliths in a single step, making it a viable method to form half and full-solid cells by hot-pressing composite cathodes on top of the SSE [195].

Hot pressing has been successfully used to produce dense Al-LLZO pellets at temperatures below conventional firing temperatures (1000°C) under 40 MPa and argon atmosphere with a typical duration of around 1 h [196]. Post-sintering of the pellet (98% theoretical density) was performed by heating at 1000°C under an air atmosphere to remove graphite contamination.

LAGP pellets (99% theoretical density) were hot pressed under moderate pressure of 56 MPa and temperature of 650°C for 1 h under an argon atmosphere [195]. A full solid cell was also produced by hot pressing, a composite cathode of LFP/LAGP onto LAGP powder followed by hot pressing lithium metal onto the resulting composite using a PEO-LiTFSI interlayer to prevent LAGP from reacting with lithium directly.

4.2.3 Spark Plasma Sintering

Success from hot-pressing of SSEs has led to using Spark plasma sintering (SPS) with heating rates and pressures (when using non-graphite dies) above those enabled by a typical hot-press. SPS is an advanced sintering technique, which uses the simultaneous application of uniaxial pressure and pulsed electrical current to densify powder compacts. Heating rates of up to 600ºC min^{-1} are more than an order of magnitude greater than that achieved with conventional sintering methods. SPS offers advantages which include faster densification, clean grain boundaries, good grain-to-grain bonding, and minimum grain growth which allows the retention of nanosized particles during sintering.

SPS has significant advantages over conventional sintering for producing pellet SSEs and for assembling solid-state batteries, with typical dwell durations of 10 minutes at peak temperature, avoiding the loss of lithium and limiting side reactions. Ta-LLZO was SPSed in graphite foil-coated TZM die alongside Ta-LLZO/LCO powder to form the electrolyte with a composite cathode [197]. The powders were pre-pressed before sintering under an argon atmosphere at 675°C and 440 MPa for 10 minutes. Post polishing the layer thicknesses of Ta-LLZO and Ta-LLZO/LCO were 1 mm and 0.2 m, respectively and compact samples had a relative density of 95%.

Similar results were obtained for a composite cathode of LTO/Ta-LLZO and LCO/Ta-Al-LLZO sintered using SPS [198,199]. In both cases, half-cells were sintered within 10 min, in temperatures ranging from 300-1000°C under a vacuum and an argon atmosphere. The LCO/Ta-Al-LLZO composite had a thickness of up to ~55 µm and a density of 95% at 750°C.

A review [14] on the applications of SPS for all solid-state batteries noted successful densification of garnet pellets, NASICON and perovskite-based SSEs with dwell periods typically less than 10 min with pressure around ~50 MPa. Cathodes are successfully sintered by SPS, promoting better interfaces between the active material and conductive carbon. All solid-state cells assembled via SPS also show increased conductivity and cycle performance over conventionally sintered stacks due to improved particle contact and low interfacial resistance.

Despite the use of SPS in other industries to produce pellets of size greater than 15 mm, there is a lack of reported large-diameter SSEs in the literature. As with hot pressing, the batched nature of the SPS limits mass production, although automation of die loading/unloading and multiple cavity dies are available. With large samples, thermal gradients may present an issue, although commercial modelling solutions are available to help mitigate this risk. The viability of SPS to sinter thin SSE layers is still questionable due to the high uniaxial forces applied.

4.2.4 Cold Sintering

Cold sintering (or CSP) is a low-temperature consolidation and sintering method that combines high applied pressure to a partially solvated ceramic mixture at low temperatures (typically <300°C) to form a sintered body. Consolidation and sintering occur through compaction and particle rearrangement followed by pressure-solution creep [200].

LATP pellets of densities up to 93% were prepared by cold sintering and post-annealing [201]. First densification was done at 120ºC, using a range of solvent mixtures (water, acetic acid, DMSO and NMP) and then followed by annealing at 650°C. Yet, pellets yielded a poor ionic

conductivity of 8.04×10^{-5} S cm^{-1} compared to bulk values reaching $>10^{-3}$ S cm^{-1} [32]. No sintering behaviour (no neck growth) occurred with NMP on its own, while water evaporated too quickly at the temperature used. Densification was successfully conducted by using a mixture of NMP with acetic acid.

Al-LLZO was cold sintered in a stainless-steel die at 50-300°C (10°C min^{-1}) with a hold at the maximum temperature under a pressure of 510 MPa for 15-60 min [202]. Sample density increased from 2.43 g cm^{-3} to 3.29 g cm^{-3} with increasing temperature (50-250°C), with density declining at 300°C to 3.15 g cm^{-3} due to rapid evaporation of the transient phase. The ionic conductivity of samples improved with density but remained poor compared to conventional sintering, this was attributed to higher porosity, lithium-proton exchange, and uncontrolled Al diffusion during the synthesis of the AL-LLZO powder.

In another example, Al-LLZO was cold sintered with water or nitric acid and pressed in a 10 mm die at 350°C, 350 MPa for 5 h [203]. Pellets were heat treated at 200°C for 6 h post sintering. Densities of up to 87.7% were achieved, and ionic conductivity remained poor which was attributed to the incongruent dissolution of Al and Li, leading to the precipitation of secondary phases rather than LLZO.

Cold sintering is promising for low temperature (and energy consumption) densification of SSEs. The key challenge in scaling up this method lies in the necessity of applying higher pressures to form larger samples. While the processes could theoretically be applied to a roller-based system and performed continuously, no works have been published in this area yet.

4.2.5 Microwave Sintering

Microwave sintering is a non-contact sintering method where volumetric heating of the sample occurs internally through microwave absorption. Heating is more efficient and faster than typical conventional heating through convection and radiation.

AL-LLZO was reactively sintered from its constituent oxides in a microwave oven at 2.45 GHz, over a range of temperatures (1000-1200°C) under nitrogen [204]. The highest relative density of 89.3% was achieved by sintering at 1200°C for 3 h.

Microwave heating is widely used across multiple industries for continuous drying processes; however, it has seen limited adoption for high-temperature processes such as sintering, due to the difficulty of preventing thermal gradients across a large bulk sample. The use of a susceptor or hybrid heating can be used to alleviate thermal gradients. When considering thin

films these gradients will be less severe. Despite the attractiveness of microwave sintering, the number of published literature on the sintering of ceramic and specifically battery ceramics such as electrolytes remains limited.

4.2.6 Ultrafast High Temperature Sintering

Ultrafast high-temperature sintering (UHS) has been reported as a novel method for rapidly sintering ceramic pellets (Figure 8) [205]. This method is a re-visit of traditional fast firing, using carbon foils under resistance heating to rapidly sinter multiple small pellets (~5 mm diameter), sandwiched between foil layers. Typical process duration is less than 30 s, reaching temperatures of up to 3000°C. Nitrogen or argon atmospheres are used to limit oxidation and degradation of carbon foils. In one case the carbon foils were replaced with tungsten, using an SPS system to meet the increased current demand [206].

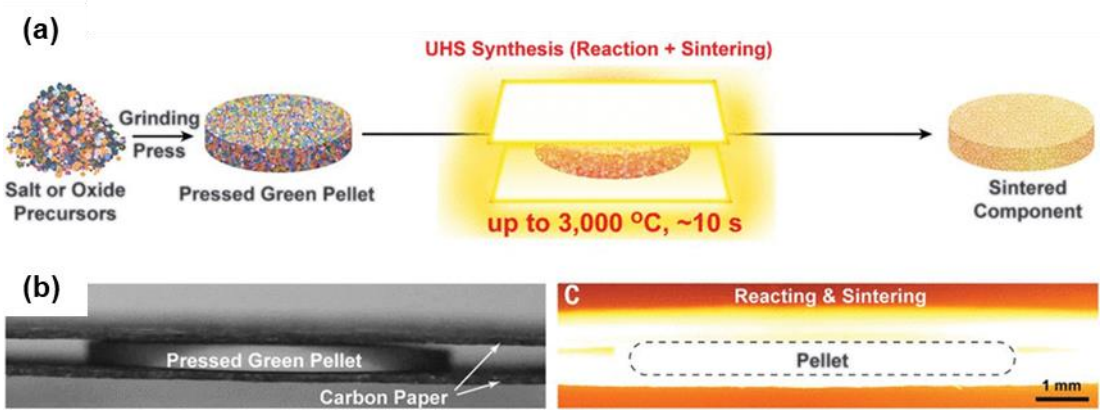

Figure 8. (a) Schematic of the UHS synthesis process, (b) Photographs of the UHS sintering setup at room temperature without applying current, and (c) at ~1500°C [205].

The method was used to sinter pellets of Ta-LLZO (~97%), LATP (>90%) and LLTO (>94%) from constituent oxides [205]. Due to very fast sintering in less than 1 min, lithium loss for Ta-LLZO samples was less than 4% compared to over 99% loss for samples sintered in a conventional furnace (Figure 9).

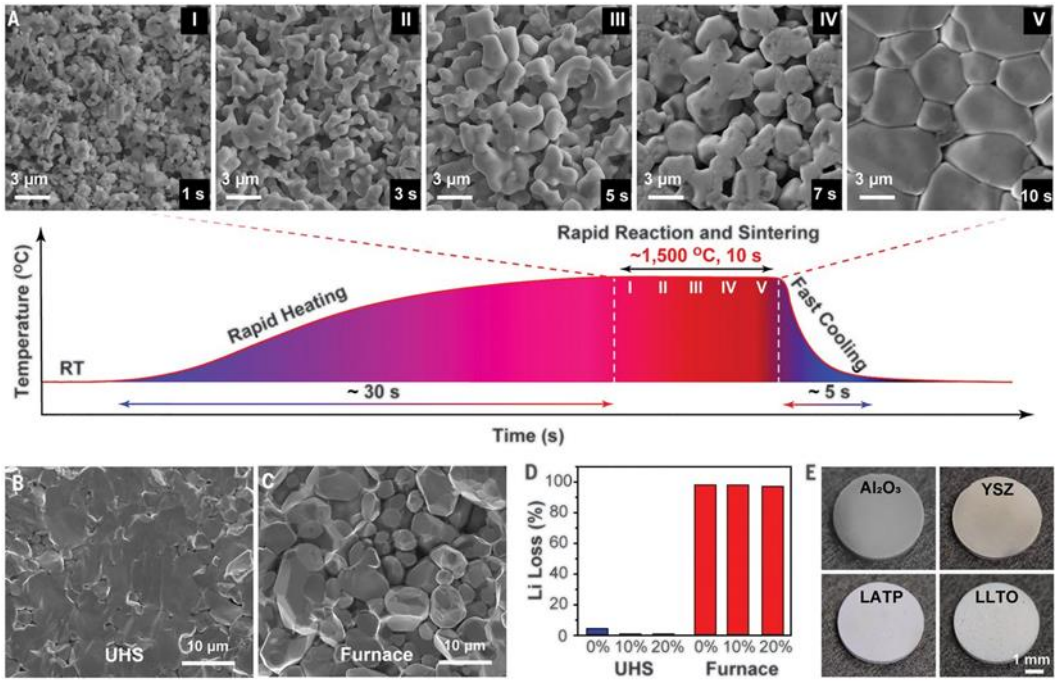

Figure 9. (a) The typical temperature profile of the UHS process. The whole process takes <1 min. The SEM images demonstrate the reaction process of the LLZTO ceramic over a 10-s isothermal hold of UHS sintering. RT, room temperature. Fracture cross-sectional SEM images of (b) UHS-sintered and (c) conventional furnace–sintered LLZTO. (d) Li loss of different LLZTO samples sintered from precursors with 0, 10, and 20% excess Li utilizing the UHS technique and a conventional furnace. (e) Pictures of various ceramics sintered by the UHS technique in ~10 s [205].

UHS was used to sinter Ta-LLZO discs (green density of 68%), reaching a relative density of 93% after 10 s of heating via the carbon felt [207]. Partial melting of the sample was observed when high currents were applied to the carbon felt.

UHS is highly attractive for sintering SSE materials due to its fast-heating rates that avoid Li loss. While fast-firing methods typically have thermal homogeneity issues with large bulk samples, pellets or thin films should not present a challenge. The current method of UHS relies on batch production. Potential adaption to continuous manufacturing with samples passing between the heater elements in succession is more attractive to mass production but it is unlikely that it would be possible to fully surround the sample with the heating strips such as in a batched operation. While the positive effects of the rapid heating rates have been displayed, potential deleterious effects such as mechanical stress from thermal shock need to be investigated, especially on larger samples. Similar methods have been used to clean the surface of LLZO electrolytes from contaminants such as Li_2CO_3 [208].

4.2.7 Flash Sintering

Under flash sintering, an electric field is applied across a ceramic sample, using a pair of electrodes, causing rapid Joule heating of the sample. Most ceramics have a negative temperature coefficient of resistivity, as the ceramic heats its resistance decreases resulting in a runaway process of increasing power dissipation unless curtailed [209].

High electric fields (1 MHz) improved the sintering of LAGP by over 40% by enhancing the crystallisation of the powder before sintering [210]. However, no significant effect was observed for the use of a high field during the sintering process itself.

LLTO was flash sintered in between two electrode plates (tungsten or platinum) under an argon atmosphere or with a 5.18% O_2 in an argon mix [211]. The furnace was ramped with a fixed voltage from 60-125 V till a flash occurred. Sintered samples had inferior conductivity to the conventionally sintered sample. Microstructural homogeneity was observed in samples with a thin band of densely sintered material surrounded by an un-sintered area.

Al-LLZO dog-bone shaped samples were flash sintered at a furnace temperature of 850°C, a DC field of 40 V cm^{-1} and a maximum current of 190 mA mm^{-2} before shutting off after 15 s [212]. A final relative density of 96.5% was achieved. A separate investigation with similar parameters (850°C, 200 mA $mm^{-2,}$ 40-100 V cm^{-1}) reported similar densities for all electric field strengths with the highest density of 92.4% reported for 60 V cm^{-1} (Figure 10) [213]. At the field strengths of >80 V cm^{-1} the formation of the lithium-deficient pyrochlore ($La_2Zr_2O_7$) was detected.

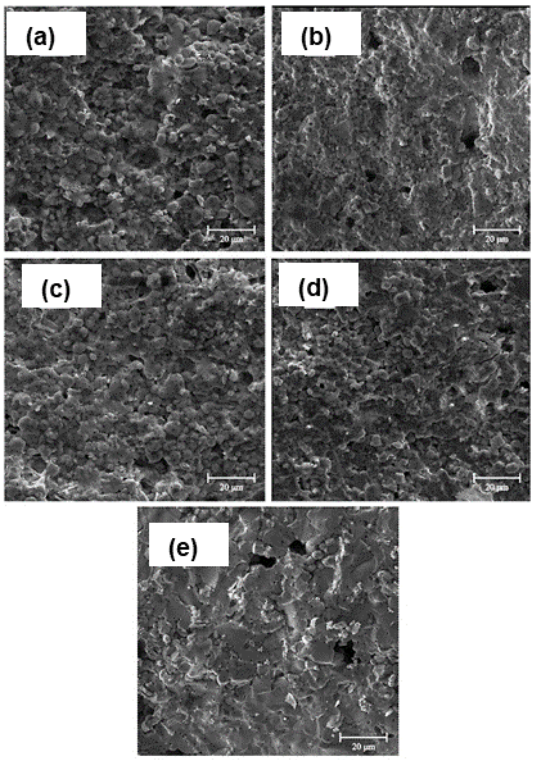

Figure 10. SEM images of the cross-sectional area of the flash sintered samples in the electric fields of (a) 40, (b) 60, (c) 80, and (d) 100 V.cm−1 (e) Conventional sintered [213] .

FS can also be used to conduct the reactive sintering of precursor compounds into the final compound in a single step. Flash sintering of Al-LLZO from its constituent oxides was conducted at 682°C, with a DC field of 50 V and a maximum of 200 mA mm^{-2}. The flash sintered sample had a relative density of 86%. The method has since been used to reactively sinter LLTO [214], boron-doped LLZO [215], and anode material LTO [216].

Retaining microstructural homogeneity even on small samples is challenging and the potential is still being investigated [209]. FS is an attractive method for processing SSEs due to its exceptionally rapid times. However, up to this point, sample sizes have remained small, and there are no reported applications of these films.

4.2.8 Photonic Sintering

Photonic sintering based on UV and IR radiation is currently widely used in the manufacturing of printed circuit boards and thin oxide films. These methods are suitable for continuous manufacturing and the handling of delicate films and are amenable to continuous manufacturing. However, these methods are not suitable for thick films due to large thermal gradients induced at the sample surface.

This rapid thermal processing method with lower heating rates than typical photonic sintering is presented in Figure 11 [217]. Tungsten halogen lamps were used to sinter an LCO/LLZO composite cathode layer (~30 µm) screen printed on top of a previously sintered LLZO layer (~500 µm, 11.5 mm in diameter). Optimisation of the heating profile was required to enable densification of the cathode layer without cracking the LLZO layer. The total optimised heating time was 7 min 15 s to a maximum temperature of 1000°C, cooling to room temperature in a further 15 s. During sintering, the thickness of the printed layer decreased to approximately 13 µm, achieving a density of 85% with macropores in the cathode layer.

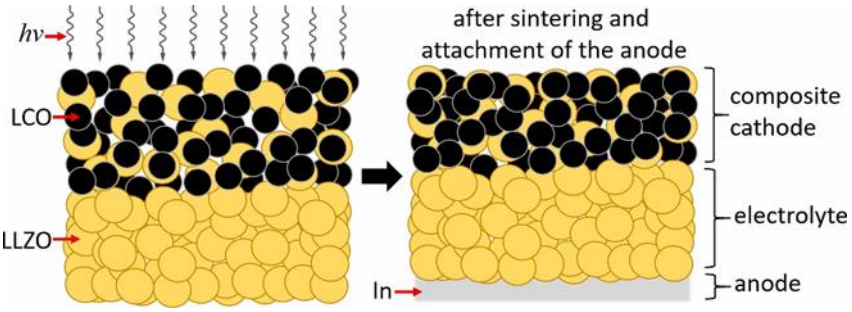

Figure 11. Schematic view of the screen-printed half-cell (left) with a composite cathode of LLZO and LCO on an LLZO electrolyte, shown in an RTP sintering process, where radiation heats the sample and causes the cathode to sinter. The half-cell with a densified cathode (right) is finally contacted with an indium metal anode [217].

4.2.9 Laser Sintering

Laser sintering is an ultrafast sintering method based on CO_2 laser scanning with the assistance of a heating stage. The method was used to sinter thick Ta-LLZO films (~300 µm) [218]. Post-sintering the films were reduced in thickness to ~150 µm with a relative density of ~96% (Figure 12). The raster pastern of the laser (6 mm s^{-1}, 300 µm between scanning lines) produced a peak and trough arrangement in the sintered sample, this could potentially be mitigated by adjustment of the laser scanning parameters or may be beneficial in increasing the contact area between the electrolyte and other SSB components. A heating bed set to 1000°C below the film was used to prevent cracking of the sample from induced thermal gradients.

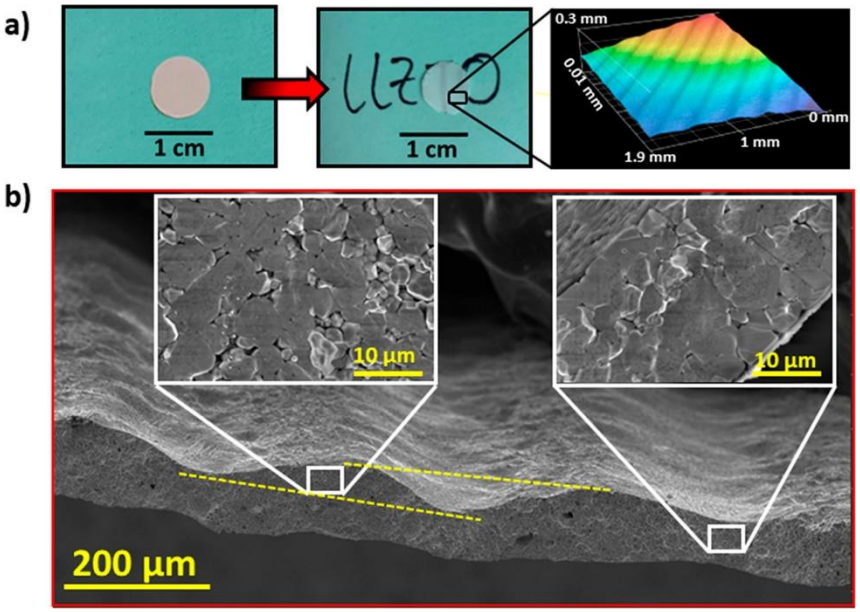

Figure 12. (a) Optical images of a pristine LLZTO film, a laser sintered film, and a 3D measurement image of the laser sintered LLZTO film; (b) SEM image of the cross-section of a laser sintered film and zoom images of a peak and a trough [218].

Laser sintering is an attractive non-contact sintering method but requires significant additional heating of the substrate to prevent thermal gradients from cracking the sample. Significant texturing of the sample surface due to the raster pattern will be detrimental, however, fine texturing is likely advantageous in enhancing surface contact as it has been proposed for 3D printed structures [219].

5 Scale-up of SSEs and Future Outlook

5.1 Forming – oxide and sulphide-based SSEs

Manufacturing of ≤25 µm thick SSEs with high-quality morphology and low interfacial impedance is desired and interest has grown since the development of commercial micro-batteries using LiPON as an SSE. All PVD processes are based on evaporating the solid coating material and transferring it onto a target substrate under vacuum conditions to create an atomic layer film. Current existing thin film deposition methods are difficult to scale up since the instruments are large, expensive, slow and operate as batch production. However, batch PVD systems such as radio frequency (RF) magnetron sputtering should not be overlooked since they are still suitable for R&D and small-scale manufacturing of bespoke micro-battery products of custom geometries such as batteries for small medical devices.

For large-scale manufacturing of SSEs, wet-forming methods seem to be the most suitable. Tape casting and screen printing are two of the most common commercial methods of high

TRL used for the preparation of ceramic films and coatings. Both methods enable the manufacturing of large areas of desired film thickness (<25 µm) [93], especially when combined with post-forming cold pressing or calendaring steps before sintering [146,147]. Both methods are also well-established technologies widely used in manufacturing free-standing films such as multi-layer ceramic capacitors (MLCC) and solid oxide fuel cells (SOFC) [220,221].

Electrophoretic deposition (EPD) is a batch process which is commercially used to produce ion-conductive Na-β″-Al_2O_3 solid electrolytes in various shapes and sizes for sodium battery development [161]. This method requires solvent and removes the need for organic binders which could allow for manufacturing high ionically conductive glass-ceramic structures [222]. By using non-polar solvents for dispersions, the method is suitable for aqueous-sensitive compositions including some crystalline and glass-ceramic oxide-type or sulphide-type SSEs. The thickness of deposited films depends on processing time under applied constant current density and a layer of 20 µm can be obtained in just 15 s [163].

In general, all solvent-free methods are attractive since they avoid the need for a drying process during manufacturing. However, in the case of powder rolling, expensive ambient and hot rolling steps are required to melt the polymer binder particles and to press the neighbouring particles together [173]. During an ambient temperature pressing step, high pressures of 20 to 500 MPa, are necessary to obtain free-standing solvent-free films [223]. Additionally, to achieve more uniform powder packing distribution, larger binder content might be required (20-50 wt.%), which might result in a prolonged binder burnout procedure.

Alternatively, dry aerosol deposition and additive manufacturing methods of lower TRL should be considered. The dry aerosol deposition could be an attractive deposition method suitable for sulphide-SSEs which are not stable against most solvents and do not require sintering.

Large-scale manufacturing of SSEs will have to depend on methods of low capital cost which might be capable of only thick film manufacturing. However, Oxide SSEs can be thinned down by calendaring followed by grinding/polishing steps after sintering to ensure low surface roughness and good contact with the electrodes [161]. In a composite approach, the cathode and SSE may be co-extruded or co-deposited as one composite material [6] allowing for the formation of stable interfaces during processing and cycling.

Viable solutions for the production chains of sulphide and oxide SSBs based on the manufacturing of SOFC and MLCC were reviewed [170] and different scenarios for SSE fabrication are presented in Figure 13. This work was followed by a systematic evaluation of

ceramic processing technologies regarding the large-scale manufacturing of SSBs [224]. Wet processing methods of low capital cost can easily be scaled up, while solvent-free deposition methods such as powder rolling, and aerosol deposition methods require further developments to reach acceptable maturity levels for mass production [224]. Based on requirements for large-scale manufacturing, tape casting and screen printing were suggested by Fraunhofer Institute in the Solid-State Battery Roadmap 2035+ as the methods of choice that would fit the SSE manufacturing strategy [30]. Yet, in the case of sulphide-based SSEs, special attention would have to be paid to additional costs associated with the need for an inert atmosphere for all processing steps from mixing to cell assembly [225–227].

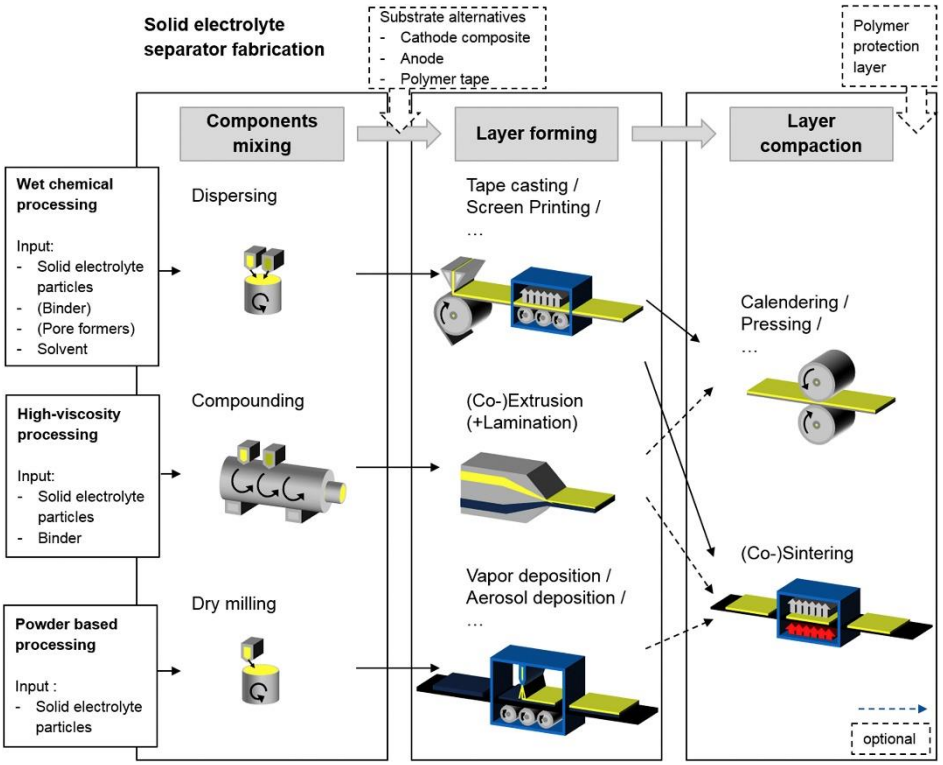

Figure 13. Process chains for solid electrolyte separator fabrication [170].

Additive manufacturing (AM) is seen as an interesting novel alternative since formulations can be either solvent-based or of low-solvent content. Independent products can be formed layer by layer into a thin green sheet of any geometry and would not require additional calendaring, just debinding and sintering. Dense layers (~10 µm, single layer) of 3D printed LLZO electrolyte have been demonstrated using a solvent-based ink formulation [219].

AM is believed to be the future for manufacturing consumer goods as 3D printing technologies are developing quickly, and are growing faster, and cheaper. One of the main challenges for AM is the limitation in high-resolution (down to nanoscale) manufacturing. However, this issue

is slowly being tackled and so far, a novel 3D printing technology, such as Ultra-Precise Deposition (UPD) was reported to print high-quality microelectronics parts with a fine resolution as low as 1 μm [228].

The electrochemical properties of the SSE will be defined by the choice of the forming method as the green body is key to the final performance. Manufacturing methods of supported and free-standing flat SSE films of any thickness are summarised in Table 2.

Table 2 Summary of forming methods for oxide- and sulphide-based SSEs.

Process	**Thickness range**	**Advantages**	**Disadvantages**
Thin film deposition methods	≤10 μm	- Deposition rate controllable down to the nanometre - High quality - Large range of stoichiometries - No post-treatment required	- Vacuum required - Slow deposition rates - High capital cost - Batch-based - Support required
Tape casting	10-240 μm	- Easy control over the thickness - Reproducible and highly homogeneous slurries can be produced - Large area covered easily with coatings	- Solvent-based - Requires solvent recovery system - Requires a calendaring step to reduce porosity - Requires high-temperature sintering
Screen-printing	5-50 μm	- Thin coating layers - Adaptable to various shape - Multiple layers can be applied - Reproducible and quick - Simple equipment	- Screen clogging may be an issue if using fine powders - Requires a binder and solvent to prepare a shear-thinning ink - Requires a calendaring step to reduce porosity
Electrophoretic Deposition (EPD)	<30 μm	- Easy control over the thickness - Easy and low cost	- Solvent-based - Requires stable dispersions - Only substrate-based coatings
Aerosol deposition	1-100 μm	- Ability to prepare thinner films - High deposition rates	- High capital cost due to high voltage us - Requires a deposition chamber
Hot powder rolling	>50 μm	- Ability to prepare solvent-free films - High deposition rates	- High capital cost due to high voltage use
Additive Manufacturing (AM)	>10 μm	- Easy control over the thickness - Large printing areas	- Printing resolution - Nozzle clogging

5.2 Sintering – oxide-based SSEs

Several techniques have been successfully used in sintering oxide SSEs to high densities and good ionic conductivities in a short time and at low temperatures [215,217,218]. Yet, the scalability of these methods is questionable.

Conventional sintering requires long processing times, however, remains a technique of low risk due to strategies that can be adapted to mitigate Li loss, for instance, the use of sintering aids. Conventional sintering has many other advantages such as low capital, higher throughput, continuous operation, and lower operating costs compared to other methods.

Truly rapid methods are hot pressing and SPS which presented good results when sintering oxide SSE pellets. Both methods can be automated and may be potentially viable for the small-scale manufacturing of coin cell-sized materials, especially when co-sintering is desired. One of the issues with using graphite dies in SPS and hot pressing is contamination and graphite diffusion into the sample resulting in poor performance of the final material [229,230]. To mitigate contamination, additional post-sintering thermal treatment steps or the use of tungsten carbide dies are required. While hot pressing and SPS are suitable for the sintering of pellet geometries their ability to process thin films is limited by the constraints of the die and uniaxial pressure. Aside from the potential challenges of trying to process thin substrates via hot pressing, the batched nature of hot pressing makes scaled-up manufacturing cost prohibitive.

Ultrafast High-temperature Sintering (UHS) is another batch processing method which uses high heating rates. The technique is pressure-less; however, the green body is sandwiched between carbon felts and Joule heating provides sufficient heat for sintering [231]. Since the sample is in contact with the heating elements, contamination is unavoidable.

Microwave sintering is a method of high interest yet remains a niche technique in ceramics processing. Microwave heating has many advantages, such as time and energy savings, high heating rates (>400 °C min^{-1}), and reduced processing time and temperature [232]. Compared to previous methods no contact with heating elements is needed and no contamination occurs. High-temperature gradients pose an issue in thicker samples [233], however, this might not be the case when sintering thin films.

Flash Sintering, while still in development, has the potential for large improvements in both the duration of the sintering process and the low temperatures required. Both contactless flash sintering and continuous contact-based flash sintering provide potentially scalable routes for large-scale manufacturing with additional potential for co-sintering. Scaling up of flash

sintering through the simultaneous connection of multiple samples is possible, however, applying consistent electrode contact to multiple samples at once provides a notable engineering challenge. A more amenable method is the use of rolling electrodes with the sample continually passing between the electrodes, this has been demonstrated on whiteware samples [234], and the difficulty of processing thin films would add additional complications. Another more applicable method of flash sintering is the use of non-contacting electrodes, with an electric arc rastered across the sample surface [235–237]. As the top electrode does not make physical contact with the sample surface, the process is suitable for continuous manufacturing and is potentially more suitable for handling delicate thin films.

Laser sintering uses localised surface heating and can introduce surface texture, which may be beneficial for improving interfacial contact, but literature is limited on this topic. Due to the localised surface heating of laser methods, co-sintering is unlikely to be viable unless thin layers are used. The method is more appropriate for sintering layers in turn followed by stacking.

Cold sintering is the lowest temperature method for densification and is based on the use of liquid phase, pressure, and heat to achieve dense ceramics. Selection of an appropriate liquid phase that does not negatively affect the sample ionic conductivity can be challenging. The use of an aqueous solvent (acidic or alkaline), particularly for the processing of lithium materials needs to be addressed due to the risk of Li^+/H^+ exchange, solutions to reverse exchange have been reviewed [111,238]. However, any post-process annealing steps or additional doping methods have associated additional process costs. The current dependence on the use of isostatic pressing to provide pressure during densification limits the method to batch production of pellets. Adaption of the method to lower pressures may enable the use of a hot calendaring approach. If cold sintering can be engineered to continuous thin-film manufacturing and its scale-up challenges are addressed, its benefits would include low volatilisation and energy consumption that would be hard to surpass with any other current sintering method.

While batch sintering has advantages in enabling gradual scaling up of manufacturing, continuous methods are more suited to labour reduction through automation. Any alternative method for conventional sintering, suitable for large-scale industrial manufacturing, would need to be easily scalable and applicable to thin films. It is worth noting that the ability to co-sinter and assemble or sinter multiple parts of a cell together adds a large additional value proposition.

Composite cathode materials may be formed by sintering the cathode with solid electrolytes at high temperatures. Co-sintering can improve the contact of cathode material and solid electrolyte [239], however, it may lead to an increase in resistance due to the chemical instability between the oxide electrolyte and interfaces [240]. Equally high-temperature sintering may result in Li loss particularly when dealing with thin films since they possess higher surface-to-volume ratios. Substantial Li loss can lead to the formation of secondary phases at the interfaces. Alongside this, a high-temperature process would introduce a higher cost than a scaled-up process.

In short, the use of sintering aids along with conventional sintering may currently be the only widely applicable option for the densification of oxide-based SSEs. With existing mitigation strategies, the possibility of reducing sintering temperature and time, or limiting excessive volatilisation of lithium, conventional sintering of SSEs or composite materials is possible.

Approaches applicable to larger samples or thin films are especially limited in literature to date, with most methods using small, thick pellets. Data available from pellet analysis is useful only for proof-of-concept; the performance of these samples does not represent a thin film optimised for electrochemical performance. Significant work needs to be conducted to optimise forming and sintering of thin oxide SSEs. The advantages, disadvantages, and mitigation strategies of all sintering methods are presented in Table 3.

Table 3 Summary of sintering methods for oxide-based SSEs.

Method	Advantages	Disadvantages	Mitigations & Considerations
		Non-batched operation feasible	
Conventional Sintering	- Non-contact - Continuous and Batch operated kilns available - Adaptable to variable sintering atmospheres	- High energy and time costs due to conventional sintering duration - Prolonged exposure to high-temperature conditions resulting in loss of volatile species	- Sintering aids can be used to reduce sintering temperature and duration - Additional doping and containment can limit volatile species loss
Microwave Sintering	- Non-contact	- Need sealed cavity - Internal to outside thermal gradients - Absorption material dependent	- Despite wide deployment for drying processes, limited off-the-shelf solutions for temperature range for sintering
Photonic Sintering	- Non-contact - Low furnace temperature requirement	- Thin films only due to low-depth penetration - May need additional heating of substrate to mitigate thermal gradients	- Applicable to thin films
Laser Sintering	- Non-contact - Low furnace temperature requirement	- Limited depth penetration without damage to the top surface -- - May need additional heating of substrate to mitigate thermal gradients - Low throughput	- Can cause surface texturing
Contactless Flash Sintering (FS)	- Sliding contact or no contact - Rapid sintering at reduced furnace temperatures	- Thermal gradients (geometry, material dependent)	- No published works on SSE materials
		Batched operation limited	
Spark Plasma Sintering (SPS)	- Large time and temperature reduction	- Die contamination. - Expensive hardware	- Automation of die loading and unloading possible
Hot Pressing	- Time and temperature reduction	- Die contamination	- Less significant time reduction than SPS but lower hardware cost
Contact Flash Sintering (FS)	- Pressureless - Rapid sintering at reduced furnace temperatures	- Requires good electrical contact to sample - Challenges in applying electrodes at a large scale or multiple samples at once - Thermal gradients (geometry, material dependent)	- Methods to make the process adaptable to continuous manufacturing have been made. - Sliding/rolling electrodes - Contactless version available
Cold sintering (CS)	- Low operation temperature	- Solvent required - Additional thermal treatment needed for burnout	- Rapidly developing area due to low energy of operation - Method may be able to be adapted to other processes to aid densification
Ultrafast High-temperature Sintering (UHS)	- Pressureless - High heating rates	- Sample in contact with heating foils, contamination potential	- Continuous manufacturing would require not having the heating coils in direct contact

5.3 Future Industrial Outlook

All research on the processing, specially forming and sintering of electrolyte materials, holds values. However, certain methods are currently more suitable for commercialisation than others.

The production of solid-state electrolytes for solid-state batteries constitutes a complex and ever-evolving field of research and development. Mitigating the risks associated with these processes for large-scale manufacturing is a crucial step in ensuring the successful transition from laboratory or pilot-scale experiments to full-scale commercial production. Given that our understanding of SSE materials is not yet fully comprehensive, reducing risks is accomplished by integrating these materials with well-established processing technologies.

Low-risk production methods are those already prevalent in the industry, utilising equipment from established manufacturers and integrators. In the ceramic industry, these methods align with those used in the production of MLCCs and SOFCs. This includes techniques such as screen printing, tape casting, and conventional sintering in batch or continuous kilns. However, it is essential to recognise the knowledge inherent in these existing industries likely needs to be transferred to solid-state battery manufacturers for seamless integration and successful production.

Research collaboration between academia and industry is essential for bridging the gap between fundamental research and large-scale production. While academic research often focuses on emerging areas and fundamental science, industry-aligned research concentrates on process optimisation. In established processes, there are significant opportunities for understanding the fundamental principles behind optimising binders and solvent pairing for enhanced processability, formation and densification of green bodies. This includes aspects like viscosity control, dispersion stability, solid loading of suspensions, and drying or curing characteristics. Improvements in sintering, aided by new technologies, dopants, and optimised conditions such as atmosphere, firing profiles, time, and temperature, are also vital.

As the limits of conventional technologies become apparent, the appetite for new technologies will grow. For instance, AM can revolutionise SSE production by enabling intricate structures and customised designs. However, challenges in forming ceramic materials need to be resolved as this technology is still in its infancy compared to forming metal or polymer components.

For large-scale SSE manufacturing, the initial stage involves establishing pilot production using available technologies and adapting them to address potential issues. This might include

conducting risk assessments to identify bottlenecks, adapting equipment from lithium polymer battery production, and exploring roll-to-roll manufacturing. Pilot scale production must meet quality standards and specifications, paving the way for further scale-up with limited process changes.

The moisture sensitivity of sulphite SSEs presents a barrier to scale-up, necessitating processing under inert atmospheres. Overcoming stability issues would alleviate these barriers. Challenges related to oxide SSEs include sintering requirements and lithium volatilisation. The commercialisation of Na-β″-Al_2O_3 SSEs in molten sodium batteries in the 1970s serves as a relevant example, showcasing the potential for overcoming similar hurdles [241,242].

Considering the supply chain for raw materials and SSE synthesis is crucial for manufacturing at scale. Availability, cost, and energy security considerations are vital factors in production planning.

The authors plan an extensive research journey focused on revalidating and optimising existing techniques. This includes evaluating different solvent and binder systems, expediting critical drying stages, and exploring the impact of sintering aids and dopants on material performance. Their commitment extends to adopting innovative sintering technologies like Flash Sintering and exploring alternative techniques like Additive Manufacturing. The exceptional design freedom inherent in AM can facilitate thin film deposition aiming for interpenetrating 3D structures of electrolytes and electrodes in solid-state batteries, removing the conventional constraints and breaking the energy-power limit of current systems. This comprehensive approach aims to advance solid-state batteries and foster their widespread application across diverse domains.

6 Conclusions

The challenges associated with the commercialisation of SSEs, including interface issues, and the overview of the prospective methods of manufacturing oxide- and sulphide-based SSEs, have been discussed.

Two main processing routes, forming and sintering methods, have been identified to produce dense SSE materials. While oxide SSEs are stable in air, sulphide SSEs are chemically unstable in ambient air, moisture, and most non-polar organic solvents. As a result, processing sulphide SSEs is currently limited to dry methods under an inert atmosphere. Small-scale manufacturing of custom thin oxide and sulphide SSE films can be achieved through

techniques like Physical Vapor Deposition (PVD) and Chemical Vapor Deposition (CVD). However, these thin film methods are likely cost-prohibitive for large-scale production.

Wet methods such as tape casting and screen printing are widely used across multiple industries to produce films, with a wide tolerance. The challenge lies in the development and optimisation of a suitable slurry or inks, especially in identifying appropriate binder and solvent systems. Additive Manufacturing (AM) is a low-energy process that provides design freedom and can offer a reduction in tooling cost in the future. However, ceramic AM technology is not as mature as polymer or metal AM, but it is steadily advancing. With ongoing research and development efforts, ceramic AM technology is expected to play an increasingly important role in the manufacturing of complex geometries and highly customized Solid-State Batteries (SSBs).

Hot-pressing and SPS have successfully densified oxide SSE pellets in short timeframes and are suitable for co-sintering and assembling all-solid-state cells. However, their low throughput rate, combined with high hardware cost makes these processes untenable for scaling up, a limitation shared by most of the pressure-dependent sintering techniques. Continuous and large-scale batched sintering processes show the most potential for successful application. Other methods such as flash sintering, laser sintering, and microwave sintering offer advantages in sintering rate over conventional furnaces, but these techniques are still in the development stages, particularly for SSE applications.

Limited information is available in the literature regarding the required level of densification, especially for film-based approaches compared to pellet approaches. Details about the duration and temperature required to achieve near-fully dense electrolytes under conventional sintering conditions are scares. However, conventional sintering still poses much lower risks compared to novel sintering methods, which require further development to achieve high TRL.

In the authors' view, large-scale manufacturing of SSEs can be accomplished through existing conventional processing methods utilised in the ceramic industry, which are inherently scalable to high production volumes. For exceptionally novel materials with unique properties such as sulphides, it might be necessary to develop specialised processing methods or extensively adapt existing ones to meet the production requirements. Collaborative efforts between industry and academic experts in materials science and manufacturing will be vital to determine appropriate paths for large-scale production of these materials.

Declaration of competing interest

The authors declare that they have no known competing financial interests or personal relationships that could have appeared to influence the work reported in this paper.

Acknowledgements

This research was partially financially supported by UK Research and Innovation's Strength in Places Fund (SIPF) Programme "Midlands Advanced Ceramics for Industry 4.0" under grant 82148.

References

[1] United Nations Environment Programme, The emissions gap report 2015:A UNEP Synthesis Report., 2015.

[2] A. Masias, J. Marcicki, W.A. Paxton, Opportunities and Challenges of Lithium Ion Batteries in Automotive Applications, ACS Energy Lett. 6 (2021) 621–630. https://doi.org/10.1021/acsenergylett.0c02584.

[3] X.-G. Yang, G. Zhang, S. Ge, C.-Y. Wang, Fast charging of lithium-ion batteries at all temperatures, Proc Natl Acad Sci U S A. 115 (2018) 7266–7271. https://doi.org/10.1073/pnas.1807115115.

[4] C.-Y. Wang, T. Liu, X.-G. Yang, S. Ge, N. V Stanley, E.S. Rountree, Y. Leng, B.D. McCarthy, Fast charging of energy-dense lithium-ion batteries, Nature. 611 (2022) 485–490. https://doi.org/10.1038/s41586-022-05281-0.

[5] M. Pasta, D. Armstrong, Z.L. Brown, J. Bu, M.R. Castell, P. Chen, A. Cocks, S.A. Corr, E.J. Cussen, E. Darnbrough, V. Deshpande, C. Doerrer, M.S. Dyer, H. El-Shinawi, N. Fleck, P. Grant, G.L. Gregory, C. Grovenor, L.J. Hardwick, J.T.S. Irvine, H.J. Lee, G. Li, E. Liberti, I. McClelland, C. Monroe, P.D. Nellist, P.R. Shearing, E. Shoko, W. Song, D.S. Jolly, C.I. Thomas, S.J. Turrell, M. Vestli, C.K. Williams, Y. Zhou, P.G. Bruce, 2020 roadmap on solid-state batteries, Journal of Physics: Energy. 2 (2020) 032008. https://doi.org/10.1088/2515-7655/ab95f4.

[6] N. Boaretto, I. Garbayo, S. Valiyaveettil-SobhanRaj, A. Quintela, C. Li, M. Casas-Cabanas, F. Aguesse, Lithium solid-state batteries: State-of-the-art and challenges for materials, interfaces and processing, J Power Sources. 502 (2021) 229919. https://doi.org/10.1016/j.jpowsour.2021.229919.

[7] A.M. Bates, Y. Preger, L. Torres-Castro, K.L. Harrison, S.J. Harris, J. Hewson, Are solid-state batteries safer than lithium-ion batteries?, Joule. 6 (2022) 742–755. https://doi.org/10.1016/j.joule.2022.02.007.

[8] A. Perea, M. Dontigny, K. Zaghib, Safety of solid-state Li metal battery: Solid polymer versus liquid electrolyte, J Power Sources. 359 (2017) 182–185. https://doi.org/10.1016/j.jpowsour.2017.05.061.

[9] W. Zhang, J. Nie, F. Li, Z.L. Wang, C. Sun, A durable and safe solid-state lithium battery with a hybrid electrolyte membrane, Nano Energy. 45 (2018) 413–419. https://doi.org/10.1016/j.nanoen.2018.01.028.

[10] Z. Sun, M. Liu, Y. Zhu, R. Xu, Z. Chen, P. Zhang, Z. Lu, P. Wang, C. Wang, Issues Concerning Interfaces with Inorganic Solid Electrolytes in All-Solid-State Lithium Metal Batteries, Sustainability (Switzerland). 14 (2022). https://doi.org/10.3390/su14159090.

[11] M. Balaish, J.C. Gonzalez-Rosillo, K.J. Kim, Y. Zhu, Z.D. Hood, J.L.M. Rupp, Processing thin but robust electrolytes for solid-state batteries, Nat Energy. 6 (2021). https://doi.org/10.1038/s41560-020-00759-5.

[12] A. Chen, C. Qu, Y. Shi, F. Shi, Manufacturing Strategies for Solid Electrolyte in Batteries, Front Energy Res. 8 (2020) 1–18. https://doi.org/10.3389/fenrg.2020.571440.

[13] R. Chen, Q. Li, X. Yu, L. Chen, H. Li, Approaching Practically Accessible Solid-State Batteries: Stability Issues Related to Solid Electrolytes and Interfaces, Chem Rev. 120 (2020) 6820–6877. https://doi.org/10.1021/acs.chemrev.9b00268.

[14] H. Zhu, J. Liu, Emerging applications of spark plasma sintering in all solid-state lithium-ion batteries and beyond, J Power Sources. 391 (2018) 10–25. https://doi.org/10.1016/j.jpowsour.2018.04.054.

[15] J. Janek, W.G. Zeier, A solid future for battery development, Nat Energy. 1 (2016) 16141. https://doi.org/10.1038/nenergy.2016.141.

[16] S. Randau, D.A. Weber, O. Kötz, R. Koerver, P. Braun, A. Weber, E. Ivers-Tiffée, T. Adermann, J. Kulisch, W.G. Zeier, F.H. Richter, J. Janek, Benchmarking the performance of all-solid-state lithium batteries, Nat Energy. 5 (2020) 259–270. https://doi.org/10.1038/s41560-020-0565-1.

[17] H. Duan, H. Zheng, Y. Zhou, B. Xu, H. Liu, Stability of garnet-type Li ion conductors: An overview, Solid State Ion. 318 (2018) 45–53. https://doi.org/10.1016/j.ssi.2017.09.018.

[18] A.B. Yaroslavtsev, Solid electrolytes: main prospects of research and development†, Russian Chemical Reviews. 85 (2016) 1255. https://doi.org/10.1070/RCR4634.

[19] E. Quartarone, P. Mustarelli, Electrolytes for solid-state lithium rechargeable batteries: recent advances and perspectives, Chem Soc Rev. 40 (2011) 2525–2540. https://doi.org/10.1039/C0CS00081G.

[20] A. Sakuda, K. Kuratani, M. Yamamoto, M. Takahashi, T. Takeuchi, H. Kobayashi, All-Solid-State Battery Electrode Sheets Prepared by a Slurry Coating Process, J Electrochem Soc. 164 (2017) A2474. https://doi.org/10.1149/2.0951712jes.

[21] Y. Meesala, A. Jena, H. Chang, R.-S. Liu, Recent Advancements in Li-Ion Conductors for All-Solid-State Li-Ion Batteries, ACS Energy Lett. 2 (2017) 2734–2751. https://doi.org/10.1021/acsenergylett.7b00849.

[22] Y.-C. Jung, M.-S. Park, D.-H. Kim, M. Ue, A. Eftekhari, D.-W. Kim, Room-Temperature Performance of Poly(Ethylene Ether Carbonate)-Based Solid Polymer Electrolytes for All-Solid-State Lithium Batteries, Sci Rep. 7 (2017) 17482. https://doi.org/10.1038/s41598-017-17697-0.

[23] J. Nanda, C. Wang, P. Liu, Frontiers of solid-state batteries, MRS Bull. 43 (2018) 740–745. https://doi.org/DOI: 10.1557/mrs.2018.234.

[24] Y.-S. Hu, Batteries: Getting solid, Nat Energy. 1 (2016) 16042. https://doi.org/10.1038/nenergy.2016.42.

[25] C. Sedlmeier, T. Kutsch, R. Schuster, L. Hartmann, R. Bublitz, M. Tominac, M. Bohn, H.A. Gasteiger, From Powder to Sheets: A Comparative Electrolyte Study for Slurry-Based Processed Solid Electrolyte/Binder-Sheets as Separators in All-Solid-State Batteries, J Electrochem Soc. 169 (2022) 070508. https://doi.org/10.1149/1945-7111/ac7e76.

[26] T. Yu, X. Yang, R. Yang, X. Bai, G. Xu, S. Zhao, Y. Duan, Y. Wu, J. Wang, Progress and perspectives on typical inorganic solid-state electrolytes, J Alloys Compd. 885 (2021). https://doi.org/10.1016/j.jallcom.2021.161013.

[27] M.-J. Uddin, S.-J. Cho, Reassessing the bulk ionic conductivity of solid-state electrolytes, Sustain Energy Fuels. 2 (2018) 1458–1462. https://doi.org/10.1039/C8SE00139A.

[28] J. Wan, J. Xie, X. Kong, Z. Liu, K. Liu, F. Shi, A. Pei, H. Chen, W. Chen, J. Chen, X. Zhang, L. Zong, J. Wang, L.-Q. Chen, J. Qin, Y. Cui, Ultrathin, flexible, solid polymer composite electrolyte enabled with aligned nanoporous host for lithium batteries, Nat Nanotechnol. 14 (2019) 705–711. https://doi.org/10.1038/s41565-019-0465-3.

[29] S. Liang, W. Yan, X. Wu, Y. Zhang, Y. Zhu, H. Wang, Y. Wu, Gel polymer electrolytes for lithium ion batteries: Fabrication, characterization and performance, Solid State Ion. 318 (2018) 2–18. https://doi.org/10.1016/j.ssi.2017.12.023.

[30] A. Schmaltz, Thomas; Wicke, Tim; Weymann, Lukas; Voß, Philipp; Neef, Christoph; Thielmann, Solid-State Battery Roadmap 2035+, (2022) 1–112.

[31] D.Y. Oh, Y.J. Nam, K.H. Park, S.H. Jung, S.J. Cho, Y.K. Kim, Y.G. Lee, S.Y. Lee, Y.S. Jung, Excellent Compatibility of Solvate Ionic Liquids with Sulfide Solid Electrolytes: Toward Favorable Ionic Contacts in Bulk-Type All-Solid-State Lithium-Ion Batteries, Adv Energy Mater. 5 (2015). https://doi.org/10.1002/aenm.201500865.

[32] M. Hou, F. Liang, K. Chen, Y. Dai, D. Xue, Challenges and perspectives of NASICON-type solid electrolytes for all-solid-state lithium batteries, Nanotechnology. 31 (2020) 132003. https://doi.org/10.1088/1361-6528/ab5be7.

[33] W. Cao, Y. Yang, J. Deng, Y. Li, C. Cui, T. Zhang, Localization of electrons within interlayer stabilizes NASICON-type solid-state electrolyte, Mater Today Energy. 22 (2021). https://doi.org/10.1016/j.mtener.2021.100875.

[34] F.J.Q. Cortes, J.A. Lewis, J. Tippens, T.S. Marchese, M.T. McDowell, How Metallic Protection Layers Extend the Lifetime of NASICON-Based Solid-State Lithium Batteries, J Electrochem Soc. 167 (2020) 050502. https://doi.org/10.1149/2.0032005jes.

[35] K. (Kelvin) Fu, Y. Gong, B. Liu, Y. Zhu, S. Xu, Y. Yao, W. Luo, C. Wang, S.D. Lacey, J. Dai, Y. Chen, Y. Mo, E. Wachsman, L. Hu, Toward garnet electrolyte–based Li metal batteries: An ultrathin, highly effective, artificial solid-state electrolyte/metallic Li interface, Sci Adv. 3 (2023) e1601659. https://doi.org/10.1126/sciadv.1601659.

[36] J. Li, H. Luo, K. Liu, J. Zhang, H. Zhai, X. Su, J. Wu, X. Tang, G. Tan, Excellent Stability of Ga-Doped Garnet Electrolyte against Li Metal Anode via Eliminating LiGaO2 Precipitates for Advanced All-Solid-State Batteries, ACS Appl Mater Interfaces. (2023). https://doi.org/10.1021/acsami.2c21603.

[37] C. Chen, K. Wang, H. He, E. Hanc, M. Kotobuki, L. Lu, Processing and Properties of Garnet-Type Li7La3Zr2O12 Ceramic Electrolytes, Small. (2022). https://doi.org/10.1002/smll.202205550.

[38] L. Feng, L. Li, Y. Zhang, H. Peng, Y. Zou, Low temperature synthesis and ion conductivity of Li7La3Zr2O12 garnets for solid state Li ion batteries, Solid State Ion. 310 (2017) 129–133. https://doi.org/10.1016/j.ssi.2017.08.016.

[39] M. Tatsumisago, M. Nagao, A. Hayashi, Recent development of sulfide solid electrolytes and interfacial modification for all-solid-state rechargeable lithium batteries, Journal of Asian Ceramic Societies. 1 (2013) 17–25. https://doi.org/10.1016/j.jascer.2013.03.005.

[40] W.G. Suci, H.K. Aliwarga, Y.R. Azinuddin, R.B. Setyawati, K.N.R. Stulasti, A. Purwanto, Review of various sulfide electrolyte types for solid-state lithium-ion batteries, Open Engineering. 12 (2022) 409–423. https://doi.org/10.1515/eng-2022-0043.

[41] D. Chang, K. Oh, S.J. Kim, K. Kang, Super-Ionic Conduction in Solid-State Li7P3S11-Type Sulfide Electrolytes, Chemistry of Materials. 30 (2018) 8764–8770. https://doi.org/10.1021/acs.chemmater.8b03000.

[42] A. Hayashi, S. Hama, H. Morimoto, M. Tatsumisago, T. Minami, Preparation of Li2S–P2S5 Amorphous Solid Electrolytes by Mechanical Milling, Journal of the American Ceramic Society. 84 (2001) 477–479. https://doi.org/https://doi.org/10.1111/j.1151-2916.2001.tb00685.x.

[43] J.A. Dawson, M.S. Islam, A Nanoscale Design Approach for Enhancing the Li-Ion Conductivity of the Li10GeP2S12 Solid Electrolyte, ACS Mater Lett. 4 (2022) 424–431. https://doi.org/10.1021/acsmaterialslett.1c00766.

[44] Y.J. Choi, S.I. Kim, M. Son, J.W. Lee, D.H. Lee, Cl- and Al-Doped Argyrodite Solid Electrolyte Li6PS5Cl for All-Solid-State Lithium Batteries with Improved Ionic Conductivity, Nanomaterials. 12 (2022). https://doi.org/10.3390/nano12244355.

[45] A. Hayashi, R. Komiya, M. Tatsumisago, T. Minami, Characterization of Li 2 S-SiS 2-Li 3 MO 3 (M=B, Al, Ga and In) oxysulfide glasses and their application to solid state lithium secondary batteries, n.d. www.elsevier.com/locate/ssi.

[46] S. Kondo, K. Takada, Y. Yamamura, SOLID STATE IONICS New lithium ion conductors based on Li2S-SiS2 system, 1992.

[47] K. Takada, N. Aotani, K. Iwamoto, S. Kondo, STATE IONICS ELSEWIER, 1995.

[48] X. Chi, Y. Zhang, F. Hao, S. Kmiec, H. Dong, R. Xu, K. Zhao, Q. Ai, T. Terlier, L. Wang, L. Zhao, L. Guo, J. Lou, H.L. Xin, S.W. Martin, Y. Yao, An electrochemically stable homogeneous glassy electrolyte formed at room temperature for all-solid-state sodium batteries, Nat Commun. 13 (2022). https://doi.org/10.1038/s41467-022-30517-y.

[49] Y. Tao, S. Chen, D. Liu, G. Peng, X. Yao, X. Xu, Lithium Superionic Conducting Oxysulfide Solid Electrolyte with Excellent Stability against Lithium Metal for All-Solid-State Cells, J Electrochem Soc. 163 (2016) A96. https://doi.org/10.1149/2.0311602jes.

[50] J.D. LaCoste, A. Zakutayev, L. Fei, A review on lithium phosphorus oxynitride, Journal of Physical Chemistry C. 125 (2021) 3651–3667. https://doi.org/10.1021/acs.jpcc.0c10001.

[51] Z. Yu, X. Zhang, C. Fu, H. Wang, M. Chen, G. Yin, H. Huo, J. Wang, Dendrites in Solid-State Batteries: Ion Transport Behavior, Advanced Characterization, and Interface Regulation, Adv Energy Mater. 11 (2021). https://doi.org/10.1002/aenm.202003250.

[52] V. Lacivita, N. Artrith, G. Ceder, Structural and Compositional Factors That Control the Li-Ion Conductivity in LiPON Electrolytes, Chemistry of Materials. 30 (2018) 7077–7090. https://doi.org/10.1021/acs.chemmater.8b02812.

[53] W. Dai, Y. Qiao, Z. Ma, T. Wang, Z. Fu, All-solid-state thin-film batteries based on lithium phosphorus oxynitrides, Materials Futures. 1 (2022) 032101. https://doi.org/10.1088/2752-5724/ac7db2.

[54] A. Sepúlveda, F. Criscuolo, B. Put, P.M. Vereecken, Effect of high temperature LiPON electrolyte in all solid state batteries, Solid State Ion. 337 (2019) 24–32. https://doi.org/https://doi.org/10.1016/j.ssi.2019.03.023.

[55] R. Zhao, G. Hu, S. Kmiec, R. Gebhardt, A. Whale, J. Wheaton, S.W. Martin, New Amorphous Oxy-Sulfide Solid Electrolyte Material: Anion Exchange, Electrochemical Properties, and Lithium Dendrite Suppression via in Situ Interfacial Modification, ACS

Appl Mater Interfaces. 13 (2021) 26841–26852. https://doi.org/10.1021/acsami.0c22305.

[56] K. Minami, F. Mizuno, A. Hayashi, M. Tatsumisago, Structure and properties of the 70Li2S·(30−x)P2S5·xP2O5 oxysulfide glasses and glass–ceramics, J Non Cryst Solids. 354 (2008) 370–373. https://doi.org/https://doi.org/10.1016/j.jnoncrysol.2007.07.059.

[57] R. Zhao, G. Hu, S. Kmiec, J. Wheaton, V.M. Torres, S.W. Martin, Grain-Boundary-Free Glassy Solid Electrolytes based on Sulfide Materials: Effects of Oxygen and Nitrogen Doping on Electrochemical Performance, Batter Supercaps. 5 (2022). https://doi.org/10.1002/batt.202100356.

[58] M. Martin, M. Okkema, S. Martin, Electrochemical Characterization of a Drawn Thin-Film Glassy Mixed Oxy-Sulfide-Nitride Phosphate Electrolyte for Applications in Solid-State Batteries, ECS Meeting Abstracts. MA2022-02 (2022) 530. https://doi.org/10.1149/MA2022-024530mtgabs.

[59] J. Liang, J. Luo, Q. Sun, X. Yang, R. Li, X. Sun, Recent progress on solid-state hybrid electrolytes for solid-state lithium batteries, Energy Storage Mater. 21 (2019) 308–334. https://doi.org/10.1016/j.ensm.2019.06.021.

[60] Z. Ding, J. Li, J. Li, C. An, Review—Interfaces: Key Issue to Be Solved for All Solid-State Lithium Battery Technologies, J Electrochem Soc. 167 (2020) 070541. https://doi.org/10.1149/1945-7111/ab7f84.

[61] Y. Huang, B. Shao, F. Han, Interfacial challenges in all-solid-state lithium batteries, Curr Opin Electrochem. 33 (2022) 1–8. https://doi.org/10.1016/j.coelec.2021.100933.

[62] Y. Li, J.-T. Han, C.-A. Wang, S.C. Vogel, H. Xie, M. Xu, J.B. Goodenough, Ionic distribution and conductivity in lithium garnet Li7La3Zr2O12, J Power Sources. 209 (2012) 278–281. https://doi.org/https://doi.org/10.1016/j.jpowsour.2012.02.100.

[63] C. Deviannapoorani, L. Dhivya, S. Ramakumar, R. Murugan, Lithium ion transport properties of high conductive tellurium substituted Li7La3Zr2O12 cubic lithium garnets, J Power Sources. 240 (2013) 18–25. https://doi.org/https://doi.org/10.1016/j.jpowsour.2013.03.166.

[64] N. Zhao, W. Khokhar, Z. Bi, C. Shi, X. Guo, L.Z. Fan, C.W. Nan, Solid Garnet Batteries, Joule. 3 (2019) 1190–1199. https://doi.org/10.1016/j.joule.2019.03.019.

[65] R. Murugan, V. Thangadurai, W. Weppner, Fast Lithium Ion Conduction in Garnet-Type Li7La3Zr2O12, Angewandte Chemie International Edition. 46 (2007) 7778–7781. https://doi.org/https://doi.org/10.1002/anie.200701144.

[66] Y. Zhu, X. He, Y. Mo, Origin of Outstanding Stability in the Lithium Solid Electrolyte Materials: Insights from Thermodynamic Analyses Based on First-Principles Calculations, ACS Appl Mater Interfaces. 7 (2015) 23685–23693. https://doi.org/10.1021/acsami.5b07517.

[67] W.D. Richards, L.J. Miara, Y. Wang, J.C. Kim, G. Ceder, Interface Stability in Solid-State Batteries, Chemistry of Materials. 28 (2016) 266–273. https://doi.org/10.1021/acs.chemmater.5b04082.

[68] Y. Niu, Z. Yu, Y. Zhou, J. Tang, M. Li, Z. Zhuang, Y. Yang, X. Huang, B. Tian, Constructing stable Li-solid electrolyte interphase to achieve dendrites-free solid-state battery: A nano-interlayer/Li pre-reduction strategy, Nano Res. 15 (2022) 7180–7189. https://doi.org/10.1007/s12274-022-4362-y.

[69] J. Wolfenstine, J.L. Allen, J. Sumner, J. Sakamoto, Electrical and mechanical properties of hot-pressed versus sintered LiTi2(PO4)3, Solid State Ion. 180 (2009) 961–967. https://doi.org/10.1016/j.ssi.2009.03.021.

[70] K.-Y. Yang, I.-C. Leu, K.-Z. Fung, M.-H. Hon, M.-C. Hsu, Y.-J. Hsiao, M.-C. Wang, Mechanism of the interfacial reaction between cation-deficient La0.56Li0.33TiO3 and metallic lithium at room temperature, J Mater Res. 23 (2008) 1813–1825. https://doi.org/DOI: 10.1557/JMR.2008.0255.

[71] P. Hartmann, T. Leichtweiss, M.R. Busche, M. Schneider, M. Reich, J. Sann, P. Adelhelm, J. Janek, Degradation of NASICON-Type Materials in Contact with Lithium Metal: Formation of Mixed Conducting Interphases (MCI) on Solid Electrolytes, The Journal of Physical Chemistry C. 117 (2013) 21064–21074. https://doi.org/10.1021/jp4051275.

[72] B. Wu, S. Wang, J. Lochala, D. Desrochers, B. Liu, W. Zhang, J. Yang, J. Xiao, The role of the solid electrolyte interphase layer in preventing Li dendrite growth in solid-state batteries, Energy Environ Sci. 11 (2018) 1803–1810. https://doi.org/10.1039/C8EE00540K.

[73] R. Schmuch, R. Wagner, G. Hörpel, T. Placke, M. Winter, Performance and cost of materials for lithium-based rechargeable automotive batteries, Nat Energy. 3 (2018) 267–278. https://doi.org/10.1038/s41560-018-0107-2.

[74] R. Koerver, W. Zhang, L. de Biasi, S. Schweidler, A.O. Kondrakov, S. Kolling, T. Brezesinski, P. Hartmann, W.G. Zeier, J. Janek, Chemo-mechanical expansion of lithium electrode materials – on the route to mechanically optimized all-solid-state batteries, Energy Environ Sci. 11 (2018) 2142–2158. https://doi.org/10.1039/C8EE00907D.

[75] F. Mizuno, A. Hayashi, K. Tadanaga, M. Tatsumisago, High lithium ion conducting glass-ceramics in the system Li2S-P2S5, Solid State Ion. 177 (2006) 2721–2725. https://doi.org/10.1016/j.ssi.2006.04.017.

[76] Z. Zhang, Y. Shao, B. Lotsch, Y.-S. Hu, H. Li, J. Janek, L.F. Nazar, C.-W. Nan, J. Maier, M. Armand, L. Chen, New horizons for inorganic solid state ion conductors, Energy Environ Sci. 11 (2018) 1945–1976. https://doi.org/10.1039/C8EE01053F.

[77] J. Saienga, S.W. Martin, The comparative structure, properties, and ionic conductivity of LiI + Li2S + GeS2 glasses doped with Ga2S3 and La2S3, J Non Cryst Solids. 354 (2008) 1475–1486. https://doi.org/10.1016/j.jnoncrysol.2007.08.058.

[78] C. Liu, J. Sun, P. Zheng, L. Jiang, H. Liu, J. Chai, Q. Liu, Z. Liu, Y. Zheng, X. Rui, Recent advances of non-lithium metal anode materials for solid-state lithium-ion batteries, J Mater Chem A Mater. 10 (2022) 16761–16778. https://doi.org/10.1039/D2TA03905B.

[79] T. Krauskopf, H. Hartmann, W.G. Zeier, J. Janek, Toward a Fundamental Understanding of the Lithium Metal Anode in Solid-State Batteries—An Electrochemo-Mechanical Study on the Garnet-Type Solid Electrolyte Li6.25Al0.25La3Zr2O12, ACS Appl Mater Interfaces. 11 (2019) 14463–14477. https://doi.org/10.1021/acsami.9b02537.

[80] S. Wenzel, T. Leichtweiss, D. Krüger, J. Sann, J. Janek, Interphase formation on lithium solid electrolytes—An in situ approach to study interfacial reactions by photoelectron spectroscopy, Solid State Ion. 278 (2015) 98–105. https://doi.org/https://doi.org/10.1016/j.ssi.2015.06.001.

[81] C.-L. Tsai, V. Roddatis, C.V. Chandran, Q. Ma, S. Uhlenbruck, M. Bram, P. Heitjans, O. Guillon, Li7La3Zr2O12 Interface Modification for Li Dendrite Prevention, ACS Appl Mater Interfaces. 8 (2016) 10617–10626. https://doi.org/10.1021/acsami.6b00831.

[82] Y. Suzuki, K. Kami, K. Watanabe, A. Watanabe, N. Saito, T. Ohnishi, K. Takada, R. Sudo, N. Imanishi, Transparent cubic garnet-type solid electrolyte of Al2O3-doped Li7La3Zr2O12, Solid State Ion. 278 (2015) 172–176. https://doi.org/https://doi.org/10.1016/j.ssi.2015.06.009.

[83] Y. Xiao, Y. Wang, S.-H. Bo, J.C. Kim, L.J. Miara, G. Ceder, Understanding interface stability in solid-state batteries, Nat Rev Mater. 5 (2020) 105–126. https://doi.org/10.1038/s41578-019-0157-5.

[84] A. Banerjee, H. Tang, X. Wang, J.H. Cheng, H. Nguyen, M. Zhang, D.H.S. Tan, T.A. Wynn, E.A. Wu, J.M. Doux, T. Wu, L. Ma, G.E. Sterbinsky, M.S. D'Souza, S.P. Ong, Y.S. Meng, Revealing Nanoscale Solid-Solid Interfacial Phenomena for Long-Life and High-Energy All-Solid-State Batteries, ACS Appl Mater Interfaces. 11 (2019) 43138–43145. https://doi.org/10.1021/acsami.9b13955.

[85] R. Koerver, I. Aygün, T. Leichtweiß, C. Dietrich, W. Zhang, J.O. Binder, P. Hartmann, W.G. Zeier, J. Janek, Capacity Fade in Solid-State Batteries: Interphase Formation and Chemomechanical Processes in Nickel-Rich Layered Oxide Cathodes and Lithium Thiophosphate Solid Electrolytes, Chemistry of Materials. 29 (2017) 5574–5582. https://doi.org/10.1021/acs.chemmater.7b00931.

[86] K.J. Kim, M. Balaish, M. Wadaguchi, L. Kong, J.L.M. Rupp, Solid-State Li–Metal Batteries: Challenges and Horizons of Oxide and Sulfide Solid Electrolytes and Their Interfaces, Adv Energy Mater. 11 (2021) 1–63. https://doi.org/10.1002/aenm.202002689.

[87] S. Ohta, J. Seki, Y. Yagi, Y. Kihira, T. Tani, T. Asaoka, Co-sinterable lithium garnet-type oxide electrolyte with cathode for all-solid-state lithium ion battery, J Power Sources. 265 (2014) 40–44. https://doi.org/https://doi.org/10.1016/j.jpowsour.2014.04.065.

[88] K. Nagata, T. Nanno, All solid battery with phosphate compounds made through sintering process, J Power Sources. 174 (2007) 832–837. https://doi.org/https://doi.org/10.1016/j.jpowsour.2007.06.227.

[89] R. Sudo, Y. Nakata, K. Ishiguro, M. Matsui, A. Hirano, Y. Takeda, O. Yamamoto, N. Imanishi, Interface behavior between garnet-type lithium-conducting solid electrolyte and lithium metal, Solid State Ion. 262 (2014) 151–154. https://doi.org/https://doi.org/10.1016/j.ssi.2013.09.024.

[90] M. Kotobuki, Y. Suzuki, H. Munakata, K. Kanamura, Y. Sato, K. Yamamoto, T. Yoshida, Compatibility of LiCoO2 and LiMn2O4 cathode materials for Li0.55La0.35TiO3 electrolyte to fabricate all-solid-state lithium battery, J Power Sources. 195 (2010) 5784–5788. https://doi.org/https://doi.org/10.1016/j.jpowsour.2010.03.004.

[91] M. Cengiz, H. Oh, S.-H. Lee, Lithium Dendrite Growth Suppression and Ionic Conductivity of Li2S-P2S5-P2O5 Glass Solid Electrolytes Prepared by Mechanical Milling, J Electrochem Soc. 166 (2019) A3997. https://doi.org/10.1149/2.0311916jes.

[92] S. Su, J. Ma, L. Zhao, K. Lin, Q. Li, S. Lv, F. Kang, Y.B. He, Progress and perspective of the cathode/electrolyte interface construction in all-solid-state lithium batteries, Carbon Energy. 3 (2021) 866–894. https://doi.org/10.1002/cey2.129.

[93] S.S. Zhang, A review on the separators of liquid electrolyte Li-ion batteries, J Power Sources. 164 (2007) 351–364. https://doi.org/10.1016/j.jpowsour.2006.10.065.

[94] Q. Zhang, D. Cao, Y. Ma, A. Natan, P. Aurora, H. Zhu, Sulfide-Based Solid-State Electrolytes: Synthesis, Stability, and Potential for All-Solid-State Batteries, Advanced Materials. 31 (2019). https://doi.org/10.1002/adma.201901131.

[95] M. v. Reddy, C.M. Julien, A. Mauger, K. Zaghib, Sulfide and oxide inorganic solid electrolytes for all-solid-state li batteries: A review, Nanomaterials. 10 (2020) 1–80. https://doi.org/10.3390/nano10081606.

[96] S. Wang, Y. Zhang, X. Zhang, T. Liu, Y.H. Lin, Y. Shen, L. Li, C.W. Nan, High-Conductivity Argyrodite Li 6 PS 5 Cl Solid Electrolytes Prepared via Optimized Sintering Processes for All-Solid-State Lithium-Sulfur Batteries, ACS Appl Mater Interfaces. 10 (2018) 42279–42285. https://doi.org/10.1021/acsami.8b15121.

[97] Y. Nikodimos, C.J. Huang, B.W. Taklu, W.N. Su, B.J. Hwang, Chemical stability of sulfide solid-state electrolytes: stability toward humid air and compatibility with solvents and binders, Energy Environ Sci. 15 (2022) 991–1033. https://doi.org/10.1039/d1ee03032a.

[98] K.P. Lee, N.C. Chromey, R. Culik, J.R. Barnes, P.W. Schneider, Toxicity of N-methyl-2-pyrrolidone (NMP): Teratogenic, subchronic, and two-year inhalation studies, Toxicological Sciences. 9 (1987) 222–235. https://doi.org/10.1093/toxsci/9.2.222.

[99] F.M. Courtel, S. Niketic, D. Duguay, Y. Abu-Lebdeh, I.J. Davidson, Water-soluble binders for MCMB carbon anodes for lithium-ion batteries, J Power Sources. 196 (2011) 2128–2134. https://doi.org/10.1016/j.jpowsour.2010.10.025.

[100] D. Bresser, D. Buchholz, A. Moretti, A. Varzi, S. Passerini, Alternative binders for sustainable electrochemical energy storage-the transition to aqueous electrode processing and bio-derived polymers, Energy Environ Sci. 11 (2018) 3096–3127. https://doi.org/10.1039/c8ee00640g.

[101] R.E. Mistler, E.R. Twiname, Tape Casting: Theory and Practice, Wiley, 2000.

[102] R. Kun, F. Langer, M. Delle Piane, S. Ohno, W.G. Zeier, M. Gockeln, L. Colombi Ciacchi, M. Busse, I. Fekete, Structural and Computational Assessment of the Influence of Wet-Chemical Post-Processing of the Al-Substituted Cubic Li7La3Zr2O12, ACS Appl Mater Interfaces. 10 (2018) 37188–37197. https://doi.org/10.1021/acsami.8b09789.

[103] K. Nie, S. Wu, J. Wang, X. Sun, Z. Yan, J. Qiu, Q. Yang, R. Xiao, X. Yu, H. Li, L. Chen, X. Huang, Reaction Mechanisms of Ta-Substituted Cubic Li7La3Zr2O12with Solvents during Storage, ACS Appl Mater Interfaces. 13 (2021) 38384–38393. https://doi.org/10.1021/acsami.1c10373.

[104] D.H.S. Tan, A. Banerjee, Z. Deng, E.A. Wu, H. Nguyen, J.M. Doux, X. Wang, J.H. Cheng, S.P. Ong, Y.S. Meng, Z. Chen, Enabling Thin and Flexible Solid-State Composite Electrolytes by the Scalable Solution Process, ACS Appl Energy Mater. 2 (2019) 6542–6550. https://doi.org/10.1021/acsaem.9b01111.

[105] K. Lee, S. Kim, J. Park, S.H. Park, A. Coskun, D.S. Jung, W. Cho, J.W. Choi, Selection of Binder and Solvent for Solution-Processed All-Solid-State Battery, J Electrochem Soc. 164 (2017) A2075–A2081. https://doi.org/10.1149/2.1341709jes.

[106] R. Ye, C.L. Tsai, M. Ihrig, S. Sevinc, M. Rosen, E. Dashjav, Y.J. Sohn, E. Figgemeier, M. Finsterbusch, Water-based fabrication of garnet-based solid electrolyte separators for solid-state lithium batteries, Green Chemistry. 22 (2020) 4952–4961. https://doi.org/10.1039/d0gc01009j.

[107] E. Zhen, J. Jiang, C. Lv, X. Huang, H. Xu, H. Dou, X. Zhang, Effects of binder content on low-cost solvent-free electrodes made by dry-spraying manufacturing for lithium-ion batteries, J Power Sources. 515 (2021). https://doi.org/10.1016/j.jpowsour.2021.230644.

[108] X. Huang, J. Tang, Y. Zhou, K. Rui, X. Ao, Y. Yang, B. Tian, Developing Preparation Craft Platform for Solid Electrolytes Containing Volatile Components: Experimental Study of Competition between Lithium Loss and Densification in Li7La3Zr2O12, ACS Appl Mater Interfaces. (2022). https://doi.org/10.1021/acsami.2c08442.

[109] W. Xue, Y. Yang, Q. Yang, Y. Liu, L. Wang, C. Chen, R. Cheng, The effect of sintering process on lithium ionic conductivity of Li6.4Al0.2La3Zr2O12 garnet produced by solid-state synthesis, RSC Adv. 8 (2018) 13083–13088. https://doi.org/10.1039/c8ra01329b.

[110] H. Buschmann, J. Dölle, S. Berendts, A. Kuhn, P. Bottke, M. Wilkening, P. Heitjans, A. Senyshyn, H. Ehrenberg, A. Lotnyk, V. Duppel, L. Kienle, J. Janek, Structure and dynamics of the fast lithium ion conductor “li7La3Zr2O12,” Physical Chemistry Chemical Physics. 13 (2011) 19378–19392. https://doi.org/10.1039/c1cp22108f.

[111] M. Rosen, R. Ye, M. Mann, S. Lobe, M. Finsterbusch, O. Guillon, D. Fattakhova-Rohlfing, Controlling the lithium proton exchange of LLZO to enable reproducible processing and performance optimization, J Mater Chem A Mater. 9 (2021) 4831–4840. https://doi.org/10.1039/d0ta11096e.

[112] N. Janani, C. Deviannapoorani, L. Dhivya, R. Murugan, Influence of sintering additives on densification and Li+ conductivity of Al doped Li7La3Zr2O12 lithium garnet, RSC Adv. 4 (2014) 51228–51238. https://doi.org/10.1039/c4ra08674k.

[113] H. Aono, E. Sugimoto, Y. Sadaoka, N. Imanaka, G. Adachi, Electrical property and sinterability of LiTi2(PO4)3 mixed with lithium salt (Li3PO4 or Li3BO3), Solid State Ion. 47 (1991) 257–264. https://doi.org/https://doi.org/10.1016/0167-2738(91)90247-9.

[114] E. Hanc, W. Zając, L. Lu, B. Yan, M. Kotobuki, M. Ziąbka, J. Molenda, On fabrication procedures of Li-ion conducting garnets, J Solid State Chem. 248 (2017) 51–60. https://doi.org/10.1016/j.jssc.2017.01.017.

[115] R.A. Jonson, Processing and Implementation of Substituted Li7La3Zr2O12 Solid Electrolytes in Solid-State Lithium Batteries, 2018. https://doi.org/10.7274/nk322b91r65.

[116] K. Yang, L. Chen, J. Ma, Y. He, F. Kang, Progress and perspective of Li 1 + x Al x Ti 2 -x (PO 4) 3 ceramic electrolyte in lithium batteries , InfoMat. 3 (2021) 1195–1217. https://doi.org/10.1002/inf2.12222.

[117] H. Leng, J. Nie, J. Luo, Combining cold sintering and Bi2O3-Activated liquid-phase sintering to fabricate high-conductivity Mg-doped NASICON at reduced temperatures, Journal of Materiomics. 5 (2019) 237–246. https://doi.org/10.1016/j.jmat.2019.02.005.

[118] K. Waetzig, C. Heubner, M. Kusnezoff, Reduced sintering temperatures of Li+ conductive Li1.3Al0.3Ti1.7(PO4)3 ceramics, Crystals (Basel). 10 (2020). https://doi.org/10.3390/cryst10050408.

[119] R.A. Jonson, E. Yi, F. Shen, M.C. Tucker, Optimization of Tape Casting for Fabrication of Li6.25Al0.25La3Zr2O12Sheets, Energy and Fuels. 35 (2021) 8982–8990. https://doi.org/10.1021/acs.energyfuels.1c00566.

[120] Y. Jin, P.J. McGinn, Al-doped Li7La3Zr2O12 synthesized by a polymerized complex method, J Power Sources. 196 (2011) 8683–8687. https://doi.org/10.1016/j.jpowsour.2011.05.065.

[121] R. Takano, K. Tadanaga, A. Hayashi, M. Tatsumisago, Low temperature synthesis of Al-doped Li7La3Zr 2O12 solid electrolyte by a sol-gel process, Solid State Ion. 255 (2014) 104–107. https://doi.org/10.1016/j.ssi.2013.12.006.

[122] D. Liu, W. Zhu, Z. Feng, A. Guerfi, A. Vijh, K. Zaghib, Recent progress in sulfide-based solid electrolytes for Li-ion batteries, Materials Science and Engineering: B. 213 (2016) 169–176. https://doi.org/https://doi.org/10.1016/j.mseb.2016.03.005.

[123] K. Kerman, A. Luntz, V. Viswanathan, Y.-M. Chiang, Z. Chen, Review—Practical Challenges Hindering the Development of Solid State Li Ion Batteries, J Electrochem Soc. 164 (2017) A1731–A1744. https://doi.org/10.1149/2.1571707jes.

[124] S.W. Martin, Glass and Glass-Ceramic Sulfide and Oxy-Sulfide Solid Electrolytes, in: Handbook of Solid State Batteries, WORLD SCIENTIFIC, 2015: pp. 433–501. https://doi.org/doi:10.1142/9789814651905_0014.

[125] G.O. Hartley, L. Jin, B.J. Bergner, D.S. Jolly, G.J. Rees, S. Zekoll, Z. Ning, A.T.R. Pateman, C. Holc, P. Adamson, P.G. Bruce, Is Nitrogen Present in Li3N·P2S5 Solid Electrolytes Produced by Ball Milling?, Chemistry of Materials. 31 (2019) 9993–10001. https://doi.org/10.1021/acs.chemmater.9b01853.

[126] A. Fukushima, A. Hayashi, H. Yamamura, M. Tatsumisago, Mechanochemical synthesis of high lithium ion conducting solid electrolytes in a Li2S-P2S5-Li3N system, Solid State Ion. 304 (2017) 85–89. https://doi.org/10.1016/j.ssi.2017.03.010.

[127] J. Lee, T. Lee, K. Char, K.J. Kim, J.W. Choi, Issues and Advances in Scaling up Sulfide-Based All-Solid-State Batteries, Acc Chem Res. 54 (2021) 3390–3402. https://doi.org/10.1021/acs.accounts.1c00333.

[128] A. Sakuda, A. Hayashi, M. Tatsumisago, Sulfide Solid Electrolyte with Favorable Mechanical Property for All-Solid-State Lithium Battery, Sci Rep. 3 (2013) 2261. https://doi.org/10.1038/srep02261.

[129] N. Kamaya, K. Homma, Y. Yamakawa, M. Hirayama, R. Kanno, M. Yonemura, T. Kamiyama, Y. Kato, S. Hama, K. Kawamoto, A. Mitsui, A lithium superionic conductor, Nat Mater. 10 (2011) 682–686. https://doi.org/10.1038/nmat3066.

[130] H. Muramatsu, A. Hayashi, T. Ohtomo, S. Hama, M. Tatsumisago, Structural change of Li2S–P2S5 sulfide solid electrolytes in the atmosphere, Solid State Ion. 182 (2011) 116–119. https://doi.org/https://doi.org/10.1016/j.ssi.2010.10.013.

[131] C. Yue, J. Li, L. Lin, Fabrication of Si-based three-dimensional microbatteries: A review, Frontiers of Mechanical Engineering. 12 (2017) 459–476. https://doi.org/10.1007/s11465-017-0462-x.

[132] N.A. Kyerematen, R. Hahn, Attainable Energy Density of Microbatteries, ACS Energy Lett. 3 (2018) 1172–1175. https://doi.org/10.1021/acsenergylett.8b00500.

[133] A. Jetybayeva, B. Uzakbaiuly, A. Mukanova, S.T. Myung, Z. Bakenov, Recent advancements in solid electrolytes integrated into all-solid-state 2D and 3D lithium-ion microbatteries, J Mater Chem A Mater. 9 (2021) 15140–15178. https://doi.org/10.1039/d1ta02652f.

[134] S. Kim, M. Hirayama, S. Taminato, R. Kanno, Epitaxial growth and lithium ion conductivity of lithium-oxide garnet for an all solid-state battery electrolyte, Dalton Transactions. 42 (2013) 13112–13117. https://doi.org/10.1039/C3DT51795K.

[135] J.S. Park, L. Cheng, V. Zorba, A. Mehta, J. Cabana, G. Chen, M.M. Doeff, T.J. Richardson, J.H. Park, J.-W. Son, W.-S. Hong, Effects of crystallinity and impurities on the electrical conductivity of Li–La–Zr–O thin films, Thin Solid Films. 576 (2015) 55–60. https://doi.org/https://doi.org/10.1016/j.tsf.2014.11.019.

[136] M. Rawlence, I. Garbayo, S. Buecheler, J.L.M. Rupp, On the chemical stability of post-lithiated garnet Al-stabilized Li7La3Zr2O12 solid state electrolyte thin films, Nanoscale. 8 (2016) 14746–14753. https://doi.org/10.1039/C6NR04162K.

[137] H. Katsui, T. Goto, Preparation of cubic and tetragonal Li7La3Zr2O12 film by metal organic chemical vapor deposition, Thin Solid Films. 584 (2015) 130–134. https://doi.org/10.1016/j.tsf.2014.11.094.

[138] E. Kazyak, K.H. Chen, K.N. Wood, A.L. Davis, T. Thompson, A.R. Bielinski, A.J. Sanchez, X. Wang, C. Wang, J. Sakamoto, N.P. Dasgupta, Atomic Layer Deposition of the Solid Electrolyte Garnet Li7La3Zr2O12, Chemistry of Materials. 29 (2017) 3785–3792. https://doi.org/10.1021/acs.chemmater.7b00944.

[139] D.J. Kalita, S.H. Lee, K.S. Lee, D.H. Ko, Y.S. Yoon, Ionic conductivity properties of amorphous Li–La–Zr–O solid electrolyte for thin film batteries, Solid State Ion. 229 (2012) 14–19. https://doi.org/https://doi.org/10.1016/j.ssi.2012.09.011.

[140] S. Lobe, C. Dellen, M. Finsterbusch, H.-G. Gehrke, D. Sebold, C.-L. Tsai, S. Uhlenbruck, O. Guillon, Radio frequency magnetron sputtering of Li7La3Zr2O12 thin films for solid-state batteries, J Power Sources. 307 (2016) 684–689. https://doi.org/https://doi.org/10.1016/j.jpowsour.2015.12.054.

[141] K. Tadanaga, H. Egawa, A. Hayashi, M. Tatsumisago, J. Mosa, M. Aparicio, A. Duran, Preparation of lithium ion conductive Al-doped Li7La3Zr2O12 thin films by a sol–gel process, J Power Sources. 273 (2015) 844–847. https://doi.org/https://doi.org/10.1016/j.jpowsour.2014.09.164.

[142] M. Bitzer, T. van Gestel, S. Uhlenbruck, Hans-Peter-Buchkremer, Sol-gel synthesis of thin solid Li7La3Zr2O12 electrolyte films for Li-ion batteries, Thin Solid Films. 615 (2016) 128–134. https://doi.org/https://doi.org/10.1016/j.tsf.2016.07.010.

[143] M. Hitchman, K. Jensen, Chemical vapor deposition : principles and applications, 1993.

[144] K. Kerman, A. Luntz, V. Viswanathan, Y.-M. Chiang, Z. Chen, Review—Practical Challenges Hindering the Development of Solid State Li Ion Batteries, J Electrochem Soc. 164 (2017) A1731–A1744. https://doi.org/10.1149/2.1571707jes.

[145] A. Sakuda, A. Hayashi, T. Ohtomo, S. Hama, M. Tatsumisago, All-solid-state lithium secondary batteries using LiCoO2 particles with pulsed laser deposition coatings of

Li2S-P 2S5 solid electrolytes, J Power Sources. 196 (2011) 6735–6741. https://doi.org/10.1016/j.jpowsour.2010.10.103.

[146] E. Yi, W. Wang, J. Kieffer, R.M. Laine, Flame made nanoparticles permit processing of dense, flexible, Li+ conducting ceramic electrolyte thin films of cubic-Li7La3Zr2O12 (c-LLZO), J Mater Chem A Mater. 4 (2016) 12947–12954. https://doi.org/10.1039/c6ta04492a.

[147] E. Yi, W. Wang, J. Kieffer, R.M. Laine, Key parameters governing the densification of cubic-Li7La3Zr2O12 Li+ conductors, J Power Sources. 352 (2017) 156–164. https://doi.org/10.1016/j.jpowsour.2017.03.126.

[148] E.J. Cheng, T. Kimura, M. Shoji, H. Ueda, H. Munakata, K. Kanamura, Ceramic-Based Flexible Sheet Electrolyte for Li Batteries, ACS Appl Mater Interfaces. 12 (2020) 10382–10388. https://doi.org/10.1021/acsami.9b21251.

[149] J. Xu, L. Liu, N. Yao, F. Wu, H. Li, L. Chen, Liquid-involved synthesis and processing of sulfide-based solid electrolytes, electrodes, and all-solid-state batteries, Mater Today Nano. 8 (2019). https://doi.org/10.1016/j.mtnano.2019.100048.

[150] B. Emley, Y. Liang, R. Chen, C. Wu, M. Pan, Z. Fan, Y. Yao, On the quality of tape-cast thin films of sulfide electrolytes for solid-state batteries, Materials Today Physics. 18 (2021). https://doi.org/10.1016/j.mtphys.2021.100397.

[151] K. Gao, M. He, Y. Li, Y. Zhang, J. Gao, X. Li, Z. Cui, Z. Zhan, T. Zhang, Preparation of high-density garnet thin sheet electrolytes for all-solid-state Li-Metal batteries by tape-casting technique, J Alloys Compd. 791 (2019) 923–928. https://doi.org/10.1016/j.jallcom.2019.03.409.

[152] E. Yi, H. Shen, S. Heywood, J. Alvarado, D.Y. Parkinson, G. Chen, S.W. Sofie, M.M. Doeff, All-Solid-State Batteries Using Rationally Designed Garnet Electrolyte Frameworks, ACS Appl Energy Mater. 3 (2020) 170–175. https://doi.org/10.1021/acsaem.9b02101.

[153] Z. Jiang, S. Wang, X. Chen, W. Yang, X. Yao, X. Hu, Q. Han, H. Wang, Tape-Casting Li0.34La0.56TiO3 Ceramic Electrolyte Films Permit High Energy Density of Lithium-Metal Batteries, Advanced Materials. 32 (2020). https://doi.org/10.1002/adma.201906221.

[154] R.A. Jonson, P.J. McGinn, Tape casting and sintering of Li7La3Zr1.75Nb0.25Al0.1O12 with Li3BO3 additions, Solid State Ion. 323 (2018) 49–55. https://doi.org/10.1016/j.ssi.2018.05.015.

[155] R. Jiménez, A. del Campo, M.L. Calzada, J. Sanz, S.D. Kobylianska, S.O. Solopan, A.G. Belous, Lithium La 0.57 Li 0.33 TiO 3 Perovskite and Li 1.3 Al 0.3 Ti 1.7 (PO 4) 3 Li-NASICON Supported Thick Films Electrolytes Prepared by Tape Casting Method , J Electrochem Soc. 163 (2016) A1653–A1659. https://doi.org/10.1149/2.0881608jes.

[156] L. Puech, C. Cantau, P. Vinatier, G. Toussaint, P. Stevens, Elaboration and characterization of a free standing LiSICON membrane for aqueous lithium-air battery, J Power Sources. 214 (2012) 330–336. https://doi.org/10.1016/j.jpowsour.2012.04.064.

[157] E. Il'ina, S. Pershina, B. Antonov, A. Pankratov, Impact of Li3 BO3 addition on solid electrode-solid electrolyte interface in all-solid-state batteries, Materials. 14 (2021). https://doi.org/10.3390/ma14227099.

[158] S. Ohta, S. Komagata, J. Seki, T. Saeki, S. Morishita, T. Asaoka, Short communication All-solid-state lithium ion battery using garnet-type oxide and Li3BO3 solid electrolytes fabricated by screen-printing, J Power Sources. 238 (2013) 53–56. https://doi.org/10.1016/j.jpowsour.2013.02.073.

[159] C.L. Tsai, Q. Ma, C. Dellen, S. Lobe, F. Vondahlen, A. Windmüller, D. Grüner, H. Zheng, S. Uhlenbruck, M. Finsterbusch, F. Tietz, D. Fattakhova-Rohlfing, H.P. Buchkremer, O. Guillon, A garnet structure-based all-solid-state Li battery without interface modification: Resolving incompatibility issues on positive electrodes, Sustain Energy Fuels. 3 (2019) 280–291. https://doi.org/10.1039/c8se00436f.

[160] Z. Tang, J. Choi, J.L. Lorie Lopez, A.C. Co, C.J. Brooks, J.R. Sayre, J.-H. Kim, Optimization of the Li 3 BO 3 Glass Interlayer for Garnet-Based All-Solid-State Lithium–Metal Batteries , ACS Appl Energy Mater. (2022). https://doi.org/10.1021/acsaem.2c01606.

[161] T. Nestler, R. Schmid, W. Münchgesang, V. Bazhenov, J. Schilm, T. Leisegang, D.C. Meyer, Separators - Technology review: Ceramic based separators for secondary batteries, in: AIP Conf Proc, American Institute of Physics Inc., 2014: pp. 155–184. https://doi.org/10.1063/1.4878486.

[162] T. He, G. Zeng, C. Feng, X. Jian, N. Chen, Y. Han, Q. Sun, D. Chen, S.X. Dou, W. He, A solid-electrolyte-reinforced separator through single-step electrophoretic assembly

for safe high-capacity lithium ion batteries, J Power Sources. 448 (2020) 227469. https://doi.org/10.1016/j.jpowsour.2019.227469.

[163] S. Azuma, K. Aiyama, G. Kawamura, H. Muto, T. Mizushima, T. Uchikoshi, A. Matsuda, Colloidal processing of Li2S-P2S5 films fabricated via electrophoretic deposition methods and their characterization as a solid electrolyte for all solid state lithium ion batteries, Journal of the Ceramic Society of Japan. 125 (2017) 287–292. https://doi.org/10.2109/jcersj2.16205.

[164] T. Nazarenus, Y. Sun, J. Exner, J. Kita, R. Moos, Powder Aerosol Deposition as a Method to Produce Garnet-Type Solid Ceramic Electrolytes: A Study on Electrochemical Film Properties and Industrial Applications, Energy Technology. 9 (2021). https://doi.org/10.1002/ente.202100211.

[165] R. Inada, T. Okada, A. Bando, T. Tojo, Y. Sakurai, Properties of garnet-type Li6La3ZrTaO12 solid electrolyte films fabricated by aerosol deposition method, Progress in Natural Science: Materials International. 27 (2017) 350–355. https://doi.org/10.1016/j.pnsc.2017.06.002.

[166] C.-W. Ahn, J.-J. Choi, J. Ryu, B.-D. Hahn, J.-W. Kim, W.-H. Yoon, J.-H. Choi, D.-S. Park, Microstructure and Ionic Conductivity in Li7La3Zr2O12 Film Prepared by Aerosol Deposition Method, J Electrochem Soc. 162 (2015) A60. https://doi.org/10.1149/2.0411501jes.

[167] D. Hanft, J. Exner, R. Moos, Thick-films of garnet-type lithium ion conductor prepared by the Aerosol Deposition Method: The role of morphology and annealing treatment on the ionic conductivity, J Power Sources. 361 (2017) 61–69. https://doi.org/10.1016/j.jpowsour.2017.06.061.

[168] J. Shin, H. Duong, Electrochemical Performance of Dry Battery Electrode, ECS Meeting Abstracts. MA2018-01 (2018) 365. https://doi.org/10.1149/MA2018-01/3/365.

[169] W. Zaman, K.B. Hatzell, Processing and manufacturing of next generation lithium-based all solid-state batteries, Curr Opin Solid State Mater Sci. 26 (2022). https://doi.org/10.1016/j.cossms.2022.101003.

[170] J. Schnell, T. Günther, T. Knoche, C. Vieider, L. Köhler, A. Just, M. Keller, S. Passerini, G. Reinhart, All-solid-state lithium-ion and lithium metal batteries – paving the way to large-scale production, J Power Sources. 382 (2018) 160–175. https://doi.org/10.1016/j.jpowsour.2018.02.062.

[171] C.-J. Bae, R. Rao, E.J. Shrader, High performance all solid lithium sulfur battery with fast lithium ion conduction, 2018. https://patents.google.com/patent/EP2966708B1/en (accessed November 23, 2022).

[172] B. Ludwig, J. Liu, I.M. Chen, Y. Liu, W. Shou, Y. Wang, H. Pan, Understanding Interfacial-Energy-Driven Dry Powder Mixing for Solvent-Free Additive Manufacturing of Li-Ion Battery Electrodes, Adv Mater Interfaces. 4 (2017). https://doi.org/10.1002/admi.201700570.

[173] B. Ludwig, Z. Zheng, W. Shou, Y. Wang, H. Pan, Solvent-Free Manufacturing of Electrodes for Lithium-ion Batteries, Sci Rep. 6 (2016). https://doi.org/10.1038/srep23150.

[174] H. Zhuang, W. Ma, J. Xie, X. Liu, B. Li, Y. Jiang, S. Huang, Z. Chen, B. Zhao, Solvent-free synthesis of PEO/garnet composite electrolyte for high-safety all-solid-state lithium batteries, J Alloys Compd. 860 (2021). https://doi.org/10.1016/j.jallcom.2020.157915.

[175] Z. Zhang, L. Wu, D. Zhou, W. Weng, X. Yao, Flexible Sulfide Electrolyte Thin Membrane with Ultrahigh Ionic Conductivity for All-Solid-State Lithium Batteries, Nano Lett. 21 (2021) 5233–5239. https://doi.org/10.1021/acs.nanolett.1c01344.

[176] Y. Lakhdar, C. Tuck, J. Binner, A. Terry, R. Goodridge, Additive manufacturing of advanced ceramic materials, Prog Mater Sci. 116 (2021). https://doi.org/10.1016/j.pmatsci.2020.100736.

[177] C.L. Cramer, E. Ionescu, M. Graczyk-Zajac, A.T. Nelson, Y. Katoh, J.J. Haslam, L. Wondraczek, T.G. Aguirre, S. LeBlanc, H. Wang, M. Masoudi, E. Tegeler, R. Riedel, P. Colombo, M. Minary-Jolandan, Additive manufacturing of ceramic materials for energy applications: Road map and opportunities, J Eur Ceram Soc. 42 (2022) 3049–3088. https://doi.org/https://doi.org/10.1016/j.jeurceramsoc.2022.01.058.

[178] D.W. McOwen, S. Xu, Y. Gong, Y. Wen, G.L. Godbey, J.E. Gritton, T.R. Hamann, J. Dai, G.T. Hitz, L. Hu, E.D. Wachsman, 3D-Printing Electrolytes for Solid-State Batteries, Advanced Materials. 30 (2018) 1707132. https://doi.org/10.1002/adma.201707132.

[179] D.W. Richerson, Modern Ceramic Engineering, CRC Press, 2018. https://doi.org/10.1201/b18952.

[180] A.G. Sabato, M. Nuñez Eroles, S. Anelli, C.D. Sierra, J.C. Gonzalez-Rosillo, M. Torrell, A. Pesce, G. Accardo, M. Casas-Cabanas, P. López-Aranguren, A. Morata, A.

Tarancón, 3D printing of self-supported solid electrolytes made of glass-derived Li1.5Al0.5Ge1.5P3O12 for all-solid-state lithium-metal batteries, J Mater Chem A Mater. 11 (2023) 13677–13686. https://doi.org/10.1039/D3TA01435E.

[181] B. Ozkan, F. Sameni, F. Bianchi, H. Zarezadeh, S. Karmel, D.S. Engstrøm, E. Sabet, 3D printing ceramic cores for investment casting of turbine blades, using LCD screen printers: The mixture design and characterisation, J Eur Ceram Soc. 42 (2022) 658–671. https://doi.org/https://doi.org/10.1016/j.jeurceramsoc.2021.10.043.

[182] B. Ozkan, F. Sameni, A. Goulas, S. Karmel, D.S. Engstrøm, E. Sabet, Hot ceramic lithography of silica-based ceramic cores: The effect of process temperature on vat-photopolymierisation, Addit Manuf. 58 (2022) 103033. https://doi.org/https://doi.org/10.1016/j.addma.2022.103033.

[183] F. Croce, L. Persi, F. Ronci, B. Scrosati, Nanocomposite polymer electrolytes and their impact on the lithium battery technology, Solid State Ion. 135 (2000) 47–52. https://doi.org/https://doi.org/10.1016/S0167-2738(00)00329-5.

[184] R. Lu, S. Chandrasekaran, W.L. Du Frane, R.L. Landingham, M.A. Worsley, J.D. Kuntz, Complex shaped boron carbides from negative additive manufacturing, Mater Des. 148 (2018) 8–16. https://doi.org/https://doi.org/10.1016/j.matdes.2018.03.026.

[185] Y. Lakhdar, C. Tuck, J. Binner, A. Terry, R. Goodridge, Additive manufacturing of advanced ceramic materials, Prog Mater Sci. 116 (2021) 100736. https://doi.org/https://doi.org/10.1016/j.pmatsci.2020.100736.

[186] S. Zekoll, C. Marriner-Edwards, A.K.O. Hekselman, J. Kasemchainan, C. Kuss, D.E.J. Armstrong, D. Cai, R.J. Wallace, F.H. Richter, J.H.J. Thijssen, P.G. Bruce, Hybrid electrolytes with 3D bicontinuous ordered ceramic and polymer microchannels for all-solid-state batteries, Energy Environ Sci. 11 (2018) 185–201. https://doi.org/10.1039/C7EE02723K.

[187] A. Woesz, M. Rumpler, J. Stampfl, F. Varga, N. Fratzl-Zelman, P. Roschger, K. Klaushofer, P. Fratzl, Towards bone replacement materials from calcium phosphates via rapid prototyping and ceramic gelcasting, Materials Science and Engineering: C. 25 (2005) 181–186. https://doi.org/https://doi.org/10.1016/j.msec.2005.01.014.

[188] H. Yin, S. Kirihara, Y. Miyamoto, Fabrication of Ceramic Photonic Crystals with Diamond Structure for Microwave Applications, Journal of the American Ceramic

Society. 87 (2004) 598–601. https://doi.org/https://doi.org/10.1111/j.1551-2916.2004.00598.x.

[189] G. Franchin, P. Colombo, Porous Geopolymer Components Through Inverse Replica of 3D Printed Sacrificial Templates, Journal of Ceramic Science and Technology. 6 (2015) 105–112. https://doi.org/10.4416/JCST2014-00057.

[190] S. Bose, J. Darsell, M. Kintner, H. Hosick, A. Bandyopadhyay, Pore size and pore volume effects on alumina and TCP ceramic scaffolds, Materials Science and Engineering: C. 23 (2003) 479–486. https://doi.org/https://doi.org/10.1016/S0928-4931(02)00129-7.

[191] R. Detsch, F. Uhl, U. Deisinger, G. Ziegler, 3D-Cultivation of Bone Marrow Stromal Cells on Hydroxyapatite Scaffolds Fabricated by Dispense-Plotting and Negative Mould Technique, J Mater Sci Mater Med. 19 (2008) 1491–1496. https://doi.org/10.1007/s10856-007-3297-x.

[192] A. Ortona, C. D'Angelo, S. Gianella, D. Gaia, Cellular ceramics produced by rapid prototyping and replication, Mater Lett. 80 (2012) 95–98. https://doi.org/https://doi.org/10.1016/j.matlet.2012.04.050.

[193] UK Research and Innovation, Faraday Battery Challenge: Funded Projects to Date, 2021. https://www.ukri.org/wp-content/uploads/2021/10/UKRI-051021-FaradayBatteryChallengeFundedProjectsBookletSept2021.pdf (accessed April 25, 2023).

[194] S. Ramakumar, C. Deviannapoorani, L. Dhivya, L.S. Shankar, R. Murugan, Lithium garnets: Synthesis, structure, Li+ conductivity, Li+ dynamics and applications, Prog Mater Sci. 88 (2017) 325–411. https://doi.org/10.1016/j.pmatsci.2017.04.007.

[195] A. Paolella, W. Zhu, G. Bertoni, A. Perea, H. Demers, S. Savoie, G. Girard, N. Delaporte, A. Guerfi, M. Rumpel, H. Lorrmann, G.P. Demopoulos, K. Zaghib, Toward an All-Ceramic Cathode–Electrolyte Interface with Low-Temperature Pressed NASICON Li1.5Al0.5Ge1.5(PO4)3 Electrolyte, Adv Mater Interfaces. 7 (2020) 1–8. https://doi.org/10.1002/admi.202000164.

[196] E. Rangasamy, J. Wolfenstine, J. Sakamoto, The role of Al and Li concentration on the formation of cubic garnet solid electrolyte of nominal composition Li 7La 3Zr 2O 12, Solid State Ion. 206 (2012) 28–32. https://doi.org/10.1016/j.ssi.2011.10.022.

[197] A.M. Laptev, H. Zheng, M. Bram, M. Finsterbusch, O. Guillon, High-pressure field assisted sintering of half-cell for all-solid-state battery, Mater Lett. 247 (2019) 155–158. https://doi.org/10.1016/j.matlet.2019.03.109.

[198] M. Ihrig, M. Finsterbusch, C.-L. Tsai, A.M. Laptev, C. Tu, M. Bram, Y.J. Sohn, R. Ye, S. Sevinc, S. Lin, D. Fattakhova-Rohlfing, O. Guillon, Low temperature sintering of fully inorganic all-solid-state batteries – Impact of interfaces on full cell performance, J Power Sources. 482 (2021) 228905. https://doi.org/https://doi.org/10.1016/j.jpowsour.2020.228905.

[199] S.-W. Baek, J.-M. Lee, T.Y. Kim, M.-S. Song, Y. Park, Garnet related lithium ion conductor processed by spark plasma sintering for all solid state batteries, J Power Sources. 249 (2014) 197–206. https://doi.org/https://doi.org/10.1016/j.jpowsour.2013.10.089.

[200] A. Galotta, V.M. Sglavo, The cold sintering process: A review on processing features, densification mechanisms and perspectives, J Eur Ceram Soc. 41 (2021) 1–17. https://doi.org/10.1016/j.jeurceramsoc.2021.09.024.

[201] Y. Liu, J. Liu, Q. Sun, D. Wang, K.R. Adair, J. Liang, C. Zhang, L. Zhang, S. Lu, H. Huang, X. Song, X. Sun, Insight into the Microstructure and Ionic Conductivity of Cold Sintered NASICON Solid Electrolyte for Solid-State Batteries, ACS Appl Mater Interfaces. 11 (2019) 27890–27896. https://doi.org/10.1021/acsami.9b08132.

[202] Y. Zhang, A. Liu, Z. Shi, S. Ge, J. Zhang, Microstructure and ion conductivity of Al-LLZO solid electrolyte prepared by molten salt and cold sintering process, Int J Appl Ceram Technol. 19 (2022) 320–331. https://doi.org/10.1111/ijac.13873.

[203] X. Wang, J. Wang, F. Li, F. Zhu, C. Ma, Influence of cold sintering process on the structure and properties of garnet-type solid electrolytes, Ceram Int. 46 (2020) 18544–18550. https://doi.org/10.1016/j.ceramint.2020.04.160.

[204] D. Gao, R. Wu, P. Chen, T. Hong, J. Cheng, Microwave assisted reactive sintering for Al doped Li7La3Zr2O12 lithium ion solid state electrolyte, Mater Res Express. 6 (2020) 125539. https://doi.org/10.1088/2053-1591/ab62ef.

[205] C. Wang, W. Ping, Q. Bai, H. Cui, R. Hensleigh, R. Wang, A.H. Brozena, Z. Xu, J. Dai, Y. Pei, C. Zheng, G. Pastel, J. Gao, X. Wang, H. Wang, J.C. Zhao, B. Yang, X. Zheng, J. Luo, Y. Mo, B. Dunn, L. Hu, A general method to synthesize and sinter bulk ceramics

in seconds, Science (1979). 368 (2020) 521–526. https://doi.org/10.1126/science.aaz7681.

[206] J. Wu, M. kermani, D. Zhu, J. Li, Y. Lin, C. Hu, S. Grasso, Carbon free ultra-fast high temperature sintering of translucent zirconia, Scr Mater. 210 (2022). https://doi.org/10.1016/j.scriptamat.2021.114476.

[207] M. Ihrig, T.P. Mishra, W.S. Scheld, G. Häuschen, W. Rheinheimer, M. Bram, M. Finsterbusch, O. Guillon, Li7La3Zr2O12 solid electrolyte sintered by the ultrafast high-temperature method, J Eur Ceram Soc. 41 (2021) 6075–6079. https://doi.org/10.1016/j.jeurceramsoc.2021.05.041.

[208] C. Wang, H. Xie, W. Ping, J. Dai, G. Feng, Y. Yao, S. He, J. Weaver, H. Wang, K. Gaskell, L. Hu, A general, highly efficient, high temperature thermal pulse toward high performance solid state electrolyte, Energy Storage Mater. 17 (2019) 234–241. https://doi.org/10.1016/j.ensm.2018.11.007.

[209] G.M. Jones, M. Biesuz, W. Ji, S.F. John, C. Grimley, C. Manière, C.E.J. Dancer, Promoting microstructural homogeneity during flash sintering of ceramics through thermal management, MRS Bull. 46 (2021) 59–66. https://doi.org/10.1557/s43577-020-00010-2.

[210] I. Lisenker, C.R. Stoldt, Improving NASICON Sinterability through Crystallization under High-Frequency Electrical Fields, Front Energy Res. 4 (2016) 13. https://doi.org/10.3389/fenrg.2016.00013.

[211] V.L. Blair, S. v Raju, A.L. Fry, M. Kornecki, J. Wolfenstine, R.E. Brennan, Flash Sintering of Li-Ion Conducting Lithium Lanthanum Titanate for Li–Air Batteries, in: 2018.

[212] T. Clemenceau, N. Andriamady, P. Kumar M.K., A. Badran, V. Avila, K. Dahl, M. Hopkins, X. Vendrell, D. Marshall, R. Raj, Flash sintering of Li-ion conducting ceramic in a few seconds at 850 °C, Scr Mater. 172 (2019) 1–5. https://doi.org/10.1016/j.scriptamat.2019.06.038.

[213] A. Sazvar, H. Sarpoolaky, M. Golmohammad, The effects of electric field on physical properties of LLZO made by flash sintering method, Solid State Ion. 386 (2022). https://doi.org/10.1016/j.ssi.2022.116054.

[214] V. Avila, B. Yoon, R.R. Ingraci Neto, R.S. Silva, S. Ghose, R. Raj, L.M. Jesus, Reactive flash sintering of the complex oxide Li0.5La0.5TiO3 starting from an amorphous

precursor powder, Scr Mater. 176 (2020) 78–82. https://doi.org/10.1016/j.scriptamat.2019.09.037.

[215] T. Clemenceau, R. Raj, Higher conductivity of non-stoichiometric lithium lanthanum zirconate ceramics made by reactive flash synthesis, MRS Commun. 12 (2022) 201–205. https://doi.org/10.1557/s43579-022-00162-z.

[216] F. Liu, B. Bai, L. Cheng, C. Xu, Rapid synthesis of Li 4 Ti 5 O 12 as lithium-ion battery anode by reactive flash sintering , Journal of the American Ceramic Society. (2021) 1–9. https://doi.org/10.1111/jace.18086.

[217] W.S. Scheld, S. Lobe, C. Dellen, M. Ihrig, G. Häuschen, L.C. Hoff, M. Finsterbusch, S. Uhlenbruck, O. Guillon, D. Fattakhova-Rohlfing, Rapid thermal processing of garnet-based composite cathodes, J Power Sources. 545 (2022). https://doi.org/10.1016/j.jpowsour.2022.231872.

[218] E. Ramos, A. Browar, J. Roehling, J. Ye, CO2 Laser Sintering of Garnet-Type Solid-State Electrolytes, ACS Energy Lett. 7 (2022) 3392–3400. https://doi.org/10.1021/acsenergylett.2c01630.

[219] D.W. McOwen, S. Xu, Y. Gong, Y. Wen, G.L. Godbey, J.E. Gritton, T.R. Hamann, J. Dai, G.T. Hitz, L. Hu, E.D. Wachsman, 3D-Printing Electrolytes for Solid-State Batteries, Advanced Materials. 30 (2018). https://doi.org/10.1002/adma.201707132.

[220] N.P. Simonenko, N.A. Fisenko, F.S. Fedorov, T.L. Simonenko, A.S. Mokrushin, E.P. Simonenko, G. Korotcenkov, V. v. Sysoev, V.G. Sevastyanov, N.T. Kuznetsov, Printing Technologies as an Emerging Approach in Gas Sensors: Survey of Literature, Sensors. 22 (2022). https://doi.org/10.3390/s22093473.

[221] M.R. Somalu, A. Muchtar, W.R.W. Daud, N.P. Brandon, Screen-printing inks for the fabrication of solid oxide fuel cell films: A review, Renewable and Sustainable Energy Reviews. 75 (2017) 426–439. https://doi.org/10.1016/j.rser.2016.11.008.

[222] A. Mashekova, Y. Baltash, M. Yegamkulov, I. Trussov, Z. Bakenov, A. Mukanova, Polycationic doping of the LATP ceramic electrolyte for Li-ion batteries, RSC Adv. 12 (2022) 29595–29601. https://doi.org/10.1039/d2ra05782d.

[223] N. Verdier, G. Foran, D. Lepage, A. Prébé, D. Aymé-Perrot, M. Dollé, Challenges in solvent-free methods for manufacturing electrodes and electrolytes for lithium-based batteries, Polymers (Basel). 13 (2021) 1–26. https://doi.org/10.3390/polym13030323.

[224] J. Schnell, F. Tietz, C. Singer, A. Hofer, N. Billot, G. Reinhart, Prospects of production technologies and manufacturing costs of oxide-based all-solid-state lithium batteries, Energy Environ Sci. 12 (2019) 1818–1833. https://doi.org/10.1039/c8ee02692k.

[225] C. Singer, J. Schnell, G. Reinhart, Scalable Processing Routes for the Production of All-Solid-State Batteries—Modeling Interdependencies of Product and Process, Energy Technology. 9 (2021). https://doi.org/10.1002/ente.202000665.

[226] J. Schnell, H. Knörzer, A.J. Imbsweiler, G. Reinhart, Solid versus Liquid—A Bottom-Up Calculation Model to Analyze the Manufacturing Cost of Future High-Energy Batteries, Energy Technology. 8 (2020). https://doi.org/10.1002/ente.201901237.

[227] C. Singer, H.C. Töpper, F.J. Günter, G. Reinhart, Plant Technology for the Industrial Coating Process for Sulfide-Based All-Solid-State Batteries, in: Procedia CIRP, Elsevier B.V., 2021: pp. 56–61. https://doi.org/10.1016/j.procir.2021.11.010.

[228] M. Łysień, Ł. Witczak, A. Wiatrowska, K. Fiączyk, J. Gadzalińska, L. Schneider, W. Stręk, M. Karpiński, Ł. Kosior, F. Granek, P. Kowalczewski, High-resolution deposition of conductive and insulating materials at micrometer scale on complex substrates, Sci Rep. 12 (2022). https://doi.org/10.1038/s41598-022-13352-5.

[229] K. Morita, B.N. Kim, H. Yoshida, K. Hiraga, Y. Sakka, Distribution of carbon contamination in oxide ceramics occurring during spark-plasma-sintering (SPS) processing: II - Effect of SPS and loading temperatures, J Eur Ceram Soc. 38 (2018) 2596–2604. https://doi.org/10.1016/j.jeurceramsoc.2017.12.004.

[230] H. Cai, T. Yu, D. Xie, B. Sun, J. Cheng, L. Li, X. Bao, H. Zhang, Microstructure and ionic conductivities of NASICON-type Li1.3Al0.3Ti1.7(PO4)3 solid electrolytes produced by cold sintering assisted process, J Alloys Compd. 939 (2023). https://doi.org/10.1016/j.jallcom.2023.168702.

[231] M. Kermani, D. Zhu, J. Li, J. Wu, Y. Lin, Z. Dai, C. Hu, S. Grasso, Ultra-fast High-temperature Sintering (UHS) of translucent alumina, Open Ceramics. 9 (2022). https://doi.org/10.1016/j.oceram.2021.100202.

[232] L. Ćurković, R. Veseli, I. Gabelica, I. Žmak, I. Ropuš, M. Vukšić, A review of microwave-assisted sintering technique, Transactions of Famena. 45 (2021). https://doi.org/10.21278/TOF.451021220.

[233] T. Garnault, D. Bouvard, J.-M. Chaix, C. Harnois, S. Marinel, Is direct microwave heating well suited for sintering ceramics? Is Direct Microwave Heating well adapted for Sintering of Ceramics? Is Direct Microwave Heating well adapted for Sintering of Ceramics?, (n.d.). https://doi.org/10.1016/j.ceramint.2021.02.242ï.

[234] E. Sortino, J.M. Lebrun, A. Sansone, R. Raj, Continuous flash sintering, Journal of the American Ceramic Society. 101 (2018) 1432–1440. https://doi.org/10.1111/jace.15314.

[235] T. Saunders, S. Grasso, M.J. Reece, Ultrafast-Contactless Flash Sintering using Plasma Electrodes, Sci Rep. 6 (2016). https://doi.org/10.1038/srep27222.

[236] S.L. Johnson, G. Venugopal, A.T. Hunt, Flame-assisted flash sintering: A noncontact method to flash sinter coatings on conductive substrates, Journal of the American Ceramic Society. 101 (2018) 536–541. https://doi.org/10.1111/jace.15218.

[237] J. Dong, Z. Wang, X. Zhao, M. Biesuz, T. Saunders, Z. Zhang, C. Hu, S. Grasso, Contactless flash sintering based on cold plasma, Scr Mater. 175 (2020) 20–23. https://doi.org/10.1016/j.scriptamat.2019.08.039.

[238] R. Ye, M. Ihrig, N. Imanishi, M. Finsterbusch, E. Figgemeier, A Review on Li+/H+ Exchange in Garnet Solid Electrolytes: From Instability against Humidity to Sustainable Processing in Water, ChemSusChem. (2021) cssc.202101178. https://doi.org/10.1002/cssc.202101178.

[239] H. Jing, R. Peng, R.-M. Ma, J. He, Y. Zhou, Z. Yang, C.-Y. Li, Y. Liu, X. Guo, Y. Zhu, D. Wang, J. Su, C. Sun, W. Bao, M. Wang, Flexible Ultrathin Single-Crystalline Perovskite Photodetector, Nano Lett. 20 (2020) 7144–7151. https://doi.org/10.1021/acs.nanolett.0c02468.

[240] R. Wei, S. Chen, T. Gao, W. Liu, Challenges, fabrications and horizons of oxide solid electrolytes for solid-state lithium batteries, Nano Select. 2 (2021) 2256–2274. https://doi.org/10.1002/nano.202100110.

[241] J.L. Sudworth, P. Barrow, W. Dong, B. Dunn, G.C. Farrington, J.O. Thomas, Toward Commercialization of the Beta-Alumina Family of Ionic Conductors, MRS Bull. 25 (2000) 22–26. https://doi.org/10.1557/mrs2000.14.

[242] J.L. Sudworth, The sodium/nickel chloride (ZEBRA) battery, J Power Sources. 100 (2001) 149–163. https://doi.org/https://doi.org/10.1016/S0378-7753(01)00891-6.